

# The role of salinity on genome-wide DNA methylation dynamics in European sea bass gills

Eva Blondeau-Bidet<sup>1</sup>, Ghizlane Banousse<sup>2</sup>, Thibaut L'Honoré<sup>2</sup>, Emilie Farcy<sup>2</sup>, Céline Cosseau<sup>3</sup>, and Catherine Lorin-Nebel<sup>4</sup>

<sup>1</sup>CNRS

<sup>2</sup>Université de Montpellier

<sup>3</sup>Université de Perpignan Via Domitia

<sup>4</sup>University of Montpellier

April 8, 2023

## Abstract

Epigenetic modifications, like DNA methylation, generate phenotypic diversity in fish and ultimately lead to adaptive evolutionary processes. Euryhaline marine species that migrate between salinity contrasted habitats have received little attention regarding the role of salinity on whole-genome DNA methylation. Investigation of salinity-induced DNA methylation in fish will help to better understand the potential role of this process in salinity acclimation. Using whole genome bisulfite sequencing, we compared DNA methylation patterns in European sea bass (*Dicentrarchus labrax*) juveniles in seawater and after freshwater transfer. We targeted the gill as a crucial organ involved in plastic responses to environmental changes. To investigate the function of DNA methylation in gills, we performed RNAseq and assessed DNA methylome-transcriptome correlations. We showed a negative correlation between gene expression levels and DNA methylation levels in promoters, first introns and exons. A significant effect of salinity on DNA methylation dynamics with an overall DNA hypomethylation in freshwater-transferred fish compared to seawater controls was demonstrated. This suggests a role of DNA methylation changes in salinity acclimation. Genes involved in key functions as metabolism, ion transport and transepithelial permeability (junctional complexes) were differentially methylated and expressed between salinity conditions. Expression of genes involved in mitochondrial metabolism was increased as well as the expression of DNA methyltransferases 3a. This study reveals novel aspects on the link of DNA methylation and gene expression patterns.

## The role of salinity on genome-wide DNA methylation dynamics in European sea bass gills

Eva Blondeau-Bidet<sup>1</sup>, Ghizlane Banousse<sup>1</sup>, Thibaut L'Honoré<sup>1</sup>, Emilie Farcy<sup>1</sup>, Céline Cosseau<sup>2</sup>, Catherine Lorin-Nebel<sup>1,\*</sup>

<sup>1</sup>MARBEC, Univ Montpellier, CNRS, IFREMER, IRD, Montpellier, France

<sup>2</sup>IHPE, Univ Montpellier, CNRS, Ifremer, Univ. Perpignan Via Domitia, Perpignan, France

\*Catherine.lorin@umontpellier.fr

## Abstract

Epigenetic modifications, like DNA methylation, generate phenotypic diversity in fish and ultimately lead to adaptive evolutionary processes. Euryhaline marine species that migrate between salinity contrasted habitats have received little attention regarding the role of salinity on whole-genome DNA methylation. Investigation of salinity-induced DNA methylation in fish will help to better understand the potential role of this process in salinity acclimation. Using whole genome bisulfite sequencing, we compared DNA methylation patterns in

European sea bass (*Dicentrarchus labrax*) juveniles in seawater and after freshwater transfer. We targeted the gill as a crucial organ involved in plastic responses to environmental changes. To investigate the function of DNA methylation in gills, we performed RNAseq and assessed DNA methylome-transcriptome correlations. We showed a negative correlation between gene expression levels and DNA methylation levels in promoters, first introns and exons. A significant effect of salinity on DNA methylation dynamics with an overall DNA hypomethylation in freshwater-transferred fish compared to seawater controls was demonstrated. This suggests a role of DNA methylation changes in salinity acclimation. Genes involved in key functions as metabolism, ion transport and transepithelial permeability (junctional complexes) were differentially methylated and expressed between salinity conditions. Expression of genes involved in mitochondrial metabolism was increased as well as the expression of DNA methyltransferases 3a. This study reveals novel aspects on the link of DNA methylation and gene expression patterns.

## Keywords

DNA methylation, gene expression, fish, gill, salinity, ecophysiology

## 1. Introduction

Euryhaline organisms, living in transitory habitats such as coastal lagoons or estuaries, are generally characterized by a high phenotypic plasticity. Prolonged or repeated exposure to an environmental stressor leads to changes in phenotypic responses and modification in physiological performances. Salinity strongly fluctuates in transitory habitats. Fish living in these habitats must have efficient strategies and mechanisms that operate at the gene, transcript and protein levels allowing them to respond through acclimation and to adapt. Epigenetic mechanisms like DNA methylation, histone modifications and non-coding RNA play an essential role in promoting phenotypic variation through the modulation of gene expression patterns (Bird et al. 2002). In fish, DNA methylation is the most studied epigenetic modification process in which methyl groups are transferred to the cytosines of DNA by specific DNA methyltransferases. This process potentially regulates gene expression without affecting the DNA sequence (Jones 2012). In vertebrate genomes, DNA is methylated at a high rate with about 60-80% of the cytosine-phosphate guanine (CpG) dinucleotides methylated (Feng et al., 2010). However, a subset of <10% of CpGs form clusters termed CpG islands, that are often associated with genes and known to cover part of their promoter region and at least a part of one exon (Larsen et al. 1992). CpG islands are unmethylated regions, which facilitate active gene transcription. DNA methylation plays a significant role in many biological functions through the regulation of gene expression (Suzuki and Bird, 2008). According to the methylated context considered, however, DNA methylation can have a different role in the regulation of gene expression with either an activation, inhibition, or, will remain without any functional effect (Jones 2012). DNA methylation at promoter level has often been associated with gene silencing in vertebrates (Newell-Price et al. 2000). However, recent studies suggest that DNA methylation dynamics and its regulatory role in gene expression is much more complex and depends on the cell type and genomic context (Smith et al. 2020). Promoter DNA hypermethylation has for example also been associated with high transcriptional activity by several authors (Smith et al. 2020; De Larco et al. 2003). The role of DNA methylation at gene body level was less investigated. It could be involved in transcription elongation, alternative splicing or controlling alternative promoter usage (Suzuki and Bird, 2008; Maunakea et al. 2010; Jones 2012). First introns of human genes are considered as enriched in CpG islands and are thus likely involved in transcriptional regulation (Li et al. 2012). In mammals, Brenet et al. (2011) have established a negative correlation between DNA methylation and gene expression in the first exon, and this correlation was stronger than between promoter DNA methylation and gene expression. Anastasiadi et al. (2018) have shown an inverse correlation between DNA methylation in the first intron and gene expression in European sea bass muscles and testes. The functional role of DNA methylation in different genomic contexts is therefore worth considering and requires further investigations.

Environmentally-induced changes in DNA methylation play an important role in mediating phenotypic responses that provide a substrate for selection (Flores et al. 2013). Epigenetic and genetic components are known to be important for acclimation and adaptation to salinity. In euryhaline fish that switch between salinity-contrasted habitats, epigenetic mechanisms are expected to be the major mechanism of regulation

since it allows for rapid and reversible acclimation. In fish, the effect of salinity on DNA methylation has mainly been investigated in stickleback *Gasterosteus aculeatus* (Artemov et al. 2017; Metzger et Schulte 2018; Heckwolf et al. 2020) and recently in yellow croaker (*Larimichthys crocea*) (Yang et al., 2023). Using whole genome bisulfite sequencing in a marine population of stickleback, a majority of hypomethylated cytosines have been shown at a salinity of 21 ppt relative to 2 ppt, suggesting that salinity affects DNA methylation rate. Additionally, genes known to be involved in ion transport in fish were identified with changes in mRNA expression and DNA methylation (Metzger and Schulte 2018). Using a comparative approach between stickleback populations along a natural salinity cline, and gills as a target tissue, differential methylated CpG sites were associated with osmoregulatory processes, notably ion transport and channel activity as well as water homeostasis (Heckwolf et al. 2020). In the gills of brown trout (*Salmo trutta*) fed with salt-enriched diets, short-term DNA methylation changes were shown using methylation-sensitive amplified polymorphism (MSAP) (Morán et al. 2013). Studies in marine euryhaline fish species at the genome-wide scale with single base-pair resolution methods are still lacking in order to investigate the role of DNA methylation dynamics in salinity acclimation (Metzger et Schulte 2016).

The European sea bass *Dicentrarchus labrax* is a main aquaculture species in the Mediterranean area, and has recently become an important model for genetic and epigenetic studies. In this species, environmentally-induced DNA methylation has been investigated in response to temperature (Navarro-Martín et al. 2011; Anastasiadi et al. 2017). *D. labrax* lives in coastal waters and enters estuaries and coastal lagoons that serve as feeding grounds (Pickett et al. 2004. Dufour et al. 2009). *D. labrax* have also been observed in freshwater streams that are connected to the coastal lagoons or estuaries. These transitory habitats are characterized by unpredictable salinity fluctuations with salinities ranging from 0 to over 60 ppt in Mediterranean lagoons. The influence of salinity on *D. labrax* DNA methylation dynamics is still unknown. Also, the functional role of DNA methylation changes on the transcription of genes and modulation of stress response remains poorly investigated.

In this study, we provide a high-resolution analysis of DNA methylation in European sea bass using whole-genome bisulfite sequencing (WGBS) in order to address the question if a 2-week freshwater transfer affects DNA methylation patterns in the gill tissue of *D. labrax* juveniles. DNA methylation was analyzed in different genomic regions (promoters *vs* gene bodies). RNAseq was performed to explore differentially expressed genes following freshwater exposure. To determine if DNA methylation has a functional role in salinity acclimation, we investigated the correlations between gene expression and DNA methylation levels. Salinity-responsive genes identified by RNAseq exhibiting differential DNA methylation patterns were highlighted in order to identify genes or gene families whose expression could be modulated by DNA methylation dynamics.

## 2. Material and Methods

### 2.1 Sea bass husbandry and treatment

European sea bass juveniles were reared at Ifremer Station at Palavas-les-flots (Hérault, France) in recirculating seawater (SW; osmolality: 1208 mOsm.kg<sup>-1</sup>, Na<sup>+</sup>: 515 mmol.L<sup>-1</sup>, Cl<sup>-</sup>: 737 mmol.L<sup>-1</sup>) under a 12/12 h light/dark photoperiod at 20 degC. At the age of 8 months (13.59 +- 0.12 cm, 32.19 +- 2.62 g), half of the fish were transferred to brackish water (BW; osmolality: 475 mOsm kg<sup>-1</sup>) for 24 h and then transferred to dechlorinated tap fresh water (FW; osmolality: 8 mOsm.kg<sup>-1</sup>, Na<sup>+</sup>: 2 mmol.L<sup>-1</sup>, Cl<sup>-</sup>: 3.5 mmol.L<sup>-1</sup>) for two weeks. The remaining fish were transferred from SW to SW as controls. Pellet food (Le Gouessant, France) was proposed daily to fish. After the 2-week salinity challenge, 5 fish per condition were killed using a 100 ppm lethal dose of benzocaine before immediate tissue sampling.

### 2.2 Tissue sampling

For each condition, the four left gill arches were sampled in 5 fish/salinity for epigenetic analysis and stored at -80degC. In the same fish, the four right gill arches were sampled for transcriptomic analysis. They were immersed into RNAlater (Qiagen, Mississauga, ON, Canada) overnight at 4 degC and stored at -80 degC for further analyses. The experiments were conducted according to the guidelines of the European Union (directive 86/609) and of the French law (decree 87/848) regulating animal experimentation. The

experimental design has been approved by the French legal requirement concerning welfare of experimental animals (APAFIS permit no. 9045-201701068219555).

### 2.3 Genomic DNA extraction

Genomic DNA (gDNA) was isolated from a pool of the four sampled gill arches of each juvenile using a Maxwell Blood(r)16 DNA purification kit (Promega) with the following modifications: before adding proteinase K, gill arches were homogenized with 300  $\mu$ l of lysis buffer and crushed for 30 seconds at room temperature with a laboratory mill and stainless steel beads (Mixer Mill MM 400, Retsch, Germany) and then briefly centrifuged for 10 seconds. Then the manufacturer's instructions were followed for further gDNA extraction. Purity and concentration of gDNA was estimated using the Qubit dsDNA BR Assay Kit and the Qubit Fluorimeter (Thermo Scientific, Waltham, MA, USA).

### 2.4 Whole-genome bisulfite sequencing (WGBS)

Bisulfite-conversion, library construction and sequencing (Paired-end reads - 150 bp) were performed by G enome Qu ebec (Montr eal, Canada) on an Illumina HiSeq X (Illumina, San Diego, CA, USA). Quality of the metrics are indicated in Table 1S. Reads quality analysis and alignments were performed on the local Galaxy platform (<http://bioinfo.univ-perp.fr>). The quality of the reads was checked using FastQC (version 0.11.8, Andrews 2010), and MultiQC (version 1.9, Ewels et al., 2016) was used to aggregate fastQC results into a single report. Phred scores were higher than 25 for more than 90% of the reads' length for all the sequences. FastQ reads were trimmed by Trim Galore (version 0.6.3, Krueger 2012) based on Phred score below 20 and the adaptors sequences were removed from reads. Trimmed reads were mapped with Bismark (version 0.22.1, Krueger et Andrews 2011) and aligned to the reference genome of European sea bass (Tine et al. 2014) providing global methylation percentages per genomic context (CpG, ChG and CHH). Methylation was called using Bismark Meth. Extractor tool which generated BED files.

### 2.5 Genome wide methylome analysis

After visual inspection of the quality of DNA methylation profiles using the Integrative Genomics Viewer (Thorvaldsd ottir et al., 2013), we performed the analysis of the methylome at the genome's scale. In order to evaluate the global methylation level, metagene analysis was performed using deepTools (version 2.0, Ramirez et al., 2016) command "computeMatrix" to generate read abundance from all samples over genomic regions: promoter, 5'UTR exons, coding exon, first intron, internal introns (located in non-flanking regions of genes), last intron, 3'UTR exon and Transcription End Site (TES). This matrix was then used to create, using deepTools command "plotProfile", a metagene profile from 2kb upstream of the Transcription Start Site (TSS) to 2 kb downstream of the Transcription End Site (TES). The same method was used to generate a profile plot of the level of methylation across all genomic regions.

The methylation profiles of the samples were studied using the R package MethylKit (Akalın et al. 2012). The alignment BED files were first converted into a tabular file suitable for the MethylKit package using the methylextract2methylkit tool (version 0.1.0). In order to increase the power of the statistical tests, the samples were filtered according to read coverage. Bases that had less than 10X coverage and those that had greater than 99.9th percentile coverage in each sample were filtered out from the analysis to account for potential PCR bias.

Hierarchical clustering analysis and principal component analysis were performed using the "ClusterSamples" and "PCASamples" functions, respectively, of the Methylkit R package. These analyses were based on similarities in the methylation patterns of the samples from each salinity condition. A distance correlation matrix was generated with the Pearson method and the clustering was performed using the Ward method.

### 2.6 Total RNA extraction

Total RNA was extracted from the pool of four gill arches sampled in each individual. Before RNA extraction, the gills were rinsed in 1X PBS to wash out previous storage traces and a Nucleospin  RNA kit was

used to extract total RNA following the manufacturer’s instructions (Machery-Nagel, Germany). Purity and concentration of the total RNA was checked using the NanoDrop One Spectrophotometer (Thermo Scientific, Waltham, MA, USA). The integrity of RNA was assessed using the Agilent 2100 Bioanalyzer (Thermo Scientific, Waltham, MA, USA). All samples passed the quality control threshold with RNA integrity numbers  $> 7$ .

## 2.7 Transcriptome analysis

Library construction and sequencing was performed in Perpignan University (Bio-environment platform, Perpignan, France) using one Illumina NextSeq (Illumina, San Diego, CA, USA) high output flow cell. Reads were sequenced in 75 base pairs; single end reads resulting in 25 – 30 million reads per sample. Quality of the metrics are indicated in the supplementary Table 2S. Read quality analysis and alignments were performed on the local Galaxy platform (<http://bioinfo.univ-perp.fr>). Raw read quality was assessed with FastQC (Andrews 2010) and MultiQC was used to summarize FASTQC results. Phred scores were higher than 30 for more than 90% of the read’s length for all the sequences. Reads were cleaned and adaptors removed with Cutadapt (version 1.16, Marcel (2011)). Cleaned reads were mapped against the genome of European sea bass (Tine et al. 2014) using STAR (version 2.7.8a, Dobin and Gingeras 2016). FeatureCounts (Liao et al. 2014) was used to count read-mapped per transcript.

## 2.8 Correlation analysis of genome-wide DNA methylation and gene expression

In order to reveal the complex regulation of gene expression by DNA methylation, violin plots were generated with the ggplot2 R package (version 3.3.6). Correlations between DNA methylation and gene expression levels were measured using Spearman’s rank correlation coefficient. Gene expression levels were based on counts, normalized according to the DESeq2 method (Anders et Huber 2010), and then divided into deciles of an equal number of genes ranging from the least (decile 1) to the most expressed (decile 10) genes. DNA methylation levels were based on the beta-value indicated in the BED files. DNA methylation levels in specific genomic regions were represented relative to the gene expression levels.

## 2.9 Differential methylation analysis

Differential methylation analyses were performed using the DMRseq package (version 1.18.0, Korthauer 2017) with the following parameters: block = FALSE, min Num Region = 5, deltamax = 0.25, bp span = 1000, min In Span = 10, max Gap Smooth = 2500, smooth = TRUE). DMRseq output regions (grouped per 1000 bp) were considered as differentially methylated regions (DMRs) when the p-value was  $[?] 0.05$ . Distribution of DMRs across genome features (promoter, gene body, exons, introns and intergenic regions) was performed using the bedtools intersect function (Quinlan, 2014) with the position of each genomic feature from the sea bass genome annotation file (Tine et al., 2014). DMRs located between two genomic features were counted as being located in both regions. The promoter position was defined 2kb upstream the Transcription Start Site (TSS). Hyper- and hypomethylated regions were determined according to the beta value from the DMRseq output file where a positive and a negative value correspond respectively to hyper- and hypomethylation in fresh water *vs* seawater. To visualize the chromosomal distribution of the DMRs, an horizontal bar plot was generated, showing the percentage of hyper- and hypomethylated regions on all *D. labrax* chromosomes. To determine the distribution of the DMRs within the genes among different exons and introns, we compared DMRs in exons 1 to 10 and last exons of genes as well as introns 1-10 and last introns. The analysis was performed on 10 exons as this is the average number of exons in *D. labrax* genes. Genes with only one exon were not included in the analysis. The sum of hypermethylated regions in all first exons was normalized by the total length (in bp) of all first exons, then this ratio was multiplied by 100 to get a percentage. The same method was used to determine a percentage of hypo- and hypermethylated regions in the other exons and introns 1-10, as well as last introns. This method enables to compare DMR frequency and distribution between different exons and introns and prevents bias due to the difference in length among exons and introns.

## 2.10 Differential expression analysis

Estimated read counts from featureCounts were used as input to functions in the DESeq2 R package (Love et al. 2014) to generate log<sub>2</sub> differential expression fold-difference estimates. Transcripts with less than 10 reads summed across all samples were removed from the analysis. Genes with adjusted p-value less than 5% (according to the FDR method from Benjamini-Hochberg, 1995) were declared differentially expressed. A log<sub>2</sub>FoldChange value greater than zero indicates an upregulation in FW compared to SW and a log<sub>2</sub>FoldChange value less than 0 indicates a downregulation in FW compared to SW. In order to explore the variability within our experiment, hierarchical clustering and PCA were performed after Variance Stabilizing Transformation (VST) of the count data.

## 2.11 Gene ontology (GO) enrichment analysis

A R package “org.Dalabrax.org.db” specific to sea bass annotation was generated using the MakeOrgPackage function from the AnnotationForge Package v1.40.1. The R package ClusterProfiler version 4.6.0 (Yu et al. 2012) with the “org.Dalabrax.org.db” was used to analyze functional profiles of differentially methylated and expressed genes and to identify major biological functions. The functional analysis was performed using as input the differentially methylated genes (DMGs), differentially methylated promoters (DMPs) and differentially expressed genes (DEGs). A hypergeometric test was performed and enrichment p-value of gene ontology was calculated to find significantly enriched GO terms in the input list of DMGs, DMPs and DEGs. A p-value of <0.05 was set as the threshold value. DMGs, DMPs and DEGs were categorized in three categories belonging to the main GO ontologies: biological process (BP), molecular function (MF) and cellular component (CC). In order to study the differences in functional annotation according to DNA methylation, we separated the DMGs and the DMPs into 4 groups: hyper-methylated gene bodies in FW- *vs* SW-acclimated fish (GB hyper), hypo-methylated gene bodies (GB hypo), hyper-methylated promoters (PR hyper) and hypo-methylated promoters (PR hypo). We proceeded in the same way for the transcriptome by indicating genes overexpressed in FW (up FW) or in SW (up SW). The 5 GO terms of each analysis with the most significant p-values have been represented.

In order to highlight a functional link between changes in methylation and expression patterns between salinity conditions, we identified the GO terms from the methylome and transcriptome enrichment analyses. Enriched GO terms between DEGs and DMRs (in genes and promoters) were extracted and used to generate three Venn diagrams, one per GO term category: BP, MF, and CC. This enabled us to identify enriched GO terms that are common to both analyses (methylome and transcriptome).

## 2.12 Gene expression changes in different methylation and genomic contexts

In order to determine the potential role of DNA methylation changes on gene expression patterns in different genomic contexts, the proportion (percentage) of genes according to their methylation and expression pattern was calculated and represented by horizontal bar plots.

## 2.13 KEGG pathway analysis

The “enrichKEGG” function of the R package ClusterProfiler version 4.6.0 was applied to analyze biological pathways enriched in these 4 datasets with a p-value < 0.05. Only the genes differentially methylated and expressed at the promoter level, 1st exon or 1st intron were kept to carry out this analysis (number of hyper-downregulated genes = 184, hyper-upregulated = 58, hypo-downregulated = 328 and hypo-upregulated = 322). The “emaplot” function implemented in the “ClusterProfiler” package as well as the “ggplot 2” and “enrichplot” R packages were used to generate an enrichment map. The “emaplot” function organizes the enriched terms into a network with edges connecting sets of overlapping genes. Overlapping sets of genes cluster together, making it easier to identify the functional module. The 5 KEGG pathways of each dataset with the most significant p-values have been represented. The proportion of clusters in the pie chart was determined by the number of genes.

## 3. Results

### 3.1 DNA methylation patterns in contrasted salinity treatments

Sequencing of the samples yielded 1 205 785 497 bp Illumina paired-end reads, with an average of 120 578 550 paired-end reads by library. After quality control and alignment, an average of 90 866 384 (75.4%) reads per library was uniquely mapped (Table 1S) and only the uniquely aligned reads were submitted for subsequent analyses. For each sample, the bisulfite conversion efficiency was larger than 98.7 % (Table 1S). For all samples, the majority of methylated cytosines were in the CpG context. The average methylation of CpG sites was 74.38 %  $\pm$  1.97 % in the SW control group and 73.84 %  $\pm$  2.31 % in FW-exposed *D. labrax* (Fig. 1A). Even if there was no significant difference in CpG methylation levels between FW and SW samples (Mann Whitney test,  $p = 0.83$ ) (Fig. 1A), there seemed to be a trend of FW samples being less methylated than SW samples, which was confirmed in subsequent analyses (see subsection ‘The effect of freshwater transfer on DNA methylation dynamics’). DNA methylation levels were the lowest in the promoter region at the transcription start site (TSS) and the 5’UTR (untranslated region). Higher DNA methylation levels were observed in the exons and introns. Downstream the transcription end sites (TES), a slightly lower DNA methylation was measured than in gene bodies (Fig. 1A, B).

A hierarchical clustering (Fig. 2A) and a principal component analysis (PCA) (Fig. 2B) were performed from methylation level per base data, in order to identify patterns in genome-wide methylation across treatment groups and between individuals from the same condition. Fish exposed to fresh water (black circles, Fig. 2A) clustered distinctly from fish exposed to seawater (white circles) except two individuals (SW-2 and FW-4). Individual PCA based on DNA methylation patterns is shown in Fig. 2B. Principal component 1 (PC1) explained 13.6 % of the variance of the data whereas PC2 explained 12.3 %, which makes a cumulative percentage of 25.9 %. Based on their CpG methylation profiles, distinct patterns between FW and SW exposed fish were observed with FW-acclimated fish appearing at the left upper part of the component pattern plot and SW-acclimated fish at the right lower part of the component pattern plot.

### 3.2 Gene expression patterns in contrasted salinity treatments

RNAseq yielded 282 282 453 bp Illumina single-end reads, with an average of 28 228 245 single-end reads by library. After quality control and alignment, an average of 25 225 360 (89.35 %) reads per library was uniquely mapped (Table 2S) and only the uniquely aligned reads were submitted for subsequent analyses. The dendrogram obtained from VST-transformed count data showed clustering of biological replicates and separation of biological conditions (Fig. 3A). Principal component analysis (PCA) based on gene expression patterns (Fig. 3B) showed a clear clustering of samples according to salinity conditions, indicating very distinct expression patterns between salinity conditions. Striking differences between salinity treatments were observed along the PC1-axis that explained 40 % of the variance (except FW-4, that does not contribute to the first axis). Fish from both salinity treatments distributed equally along the PC2-axis that explained 21 % of the variance. Fig 1S shows the global gene expression profiles among all individuals using a heatmap.

### 3.3 Correlation analysis of gene expression and DNA methylation levels in different genomic contexts

In the promoters, gene expression levels were negatively correlated to DNA methylation levels ( $R = -0.22$ ,  $p$ -value =  $2.2e-16$ ) (Fig. 4). In the first exons, this negative correlation was even stronger ( $R = -0.42$ ,  $p$ -value =  $2.2e-16$ ) and we observed less genes with intermediate methylation levels. Most genes exhibited strong methylation levels (>60%) had low gene expression levels (from first to 3<sup>rd</sup> decile). We also observed a negative correlation between gene expression and DNA methylation levels in the first introns ( $R = -0.34$ ,  $p$ -value =  $2.2e-16$ ) with a similar pattern than in promoters. Interestingly, lower methylation levels (<40%) were observed for highly expressed genes (from 7<sup>th</sup> to 10<sup>th</sup> decile). In contrast, when considering the rest of exons and introns, no significant correlation was found between DNA methylation and gene expression levels ( $R = 0.01$ ,  $p$ -value = 0.127).

### 3.4 The effect of freshwater transfer on DNA methylation and gene expression dynamics

We identified 17 265 differentially methylated regions (DMRs) in *D. labrax* exposed to FW *vs* SW conditions (Table 3S) ( $p$ -value <0.05) and these DMRs were uniformly spread within the 24 chromosomes (Fig. 5A). 66% of the DMRs were hypomethylated ( $n = 11\ 375$ ) whereas 34% of the DMRs were hypermethylated ( $n =$

5890) in FW. The majority of the DMRs were found in genes (48 %), among them 7 % and 41 % were present in exons and introns, respectively (Fig. 5B). In genes, we identified 2367 hypermethylated regions and 4652 hypomethylated regions in FW *vs* SW conditions. Promoter and intergenic regions contained 9 % and 43 % of DMRs, respectively. In promoters, 582 DMRs were hypermethylated and 1481 were hypomethylated in FW *vs* SW (Table 3S).

Considering exons and introns (Fig. 5C, D), DMRs showed an average percentage of 73 % of hypomethylation and 27 % of hypermethylation. DMRs were less frequent in the first (0.01 %) and last (0.005%) exons (Fig. 5C). Higher percentages of DMRs were observed in the internal exons (*i. e.* exons located in non-flanking regions of genes), with an average DMR percentage by bp of 0.0173 %. We observed the same trend in the introns, with lowest percentages of DMRs observed in the first (0.0044 %) and last (0.0048 %) introns, whereas DMRs in internal introns were 1.2-1.4 times more frequent (0.0062 %).

Among the differentially methylated gene bodies and promoters, we performed an enrichment analysis of gene ontology terms (GO-terms) (Fig. 6A, Table 4S and 6S). We identified several GO-terms that were associated to actin cytoskeleton organization and regulation, as well as GO-terms associated to bicellular tight junctions. We also identified GO categories linked to mitochondrial metabolism as H<sup>+</sup>-transporting ATP synthase activity and oxidoreductase activity as well as proton channel activity (black stars, Fig. 6A). The most significant GO-terms of the DNA methylome analysis are listed in Table 4S.

A differential analysis was performed to identify gene expression patterns between FW and SW exposed fish. We found 5144 differentially expressed genes (DEGs), among which 2316 were upregulated and 2828 were downregulated (Table 5S). The enrichment analysis of GO-terms (Fig. 6B, Table 4S and 6S) identified functional categories involving genes that were upregulated in fresh water linked to mitochondrial metabolism. These include genes involved in the tricarboxylic acid (TCA) cycle (as dihydrolipoamide S-succinyltransferase *dlst*, succinate dehydrogenases *sdha*, *sdhd*, *sdhb* and mitochondrial citrate synthase precursor *cs*), genes linked to the ‘electron transport chain’, ‘electron transfer activity’ and ‘ATP biosynthetic process’. Genes linked to methionine metabolism as s-methyl-5-thioadenosine phosphorylase (*mtap*) were upregulated. We also identified upregulated genes involved in other metabolic processes (peptide metabolic process, cellular amino acid metabolic process) as well as ATPase and proton transporter activity (see next paragraph on ATPases). In contrast, genes with molecular functions linked to membrane rafts and membrane microdomains were downregulated in fresh water. The most significant GO-terms of the transcriptome analysis are listed in Table 4S.

### 3.5 Changes in DNA methylation and gene expression profiles are identified in specific gene pathways

Enrichment analyses of gene ontology terms (GO-terms) were done in both analyses (transcriptome and methylome) to identify the enriched GO terms. Venn diagrams in Fig. 7 show the numbers and percentages of unique and common GO terms between DMRs (in genes and promoters) and DEGs. For the ‘biological process’ category (Fig. 7A), the results showed 17% of common GO terms between DMRs and DMGs. Among them, we identified categories involved in metabolism as ‘carbohydrate derivative biosynthetic process’, ‘lipid biosynthesis process’ and ‘mitochondrial transport’. Concerning the ‘molecular function’ category (Fig. 7B), 14% of enriched GO terms were common between DMRs and DEGs. Among these GO terms we identified main categories involved in active ion transport, as ‘ATPase-coupled transmembrane transporter activity’. Several genes encoding for ATPases such as different subunits of Na<sup>+</sup>/K<sup>+</sup>-ATPase (*atp1a1*, *atp1a3b*) and the V-H<sup>+</sup>-ATPase (*atp6v1b2*, *atp6v1d*) were upregulated in FW and showed differential methylation patterns between salinities (Table 1). We also identified genes encoding for other main ion transporters or channels that showed differential methylation and were upregulated (as one *clcn2* paralog, *clcn3*, several K<sup>+</sup> channels: *kcnh5*, *kcnk5*, *kcnt1*) or downregulated in FW (*scn4a* Na<sup>+</sup> channel, *atp6v1e1b* subunit of V-H<sup>+</sup>-ATPase, chloride channels *cfltr* and one of the *clcn2* paralog, potassium channel *kcnma1*, and an ammonium channel *rhcg*). The gene encoding for Aquaporin 3, a glyceroporin, was strongly upregulated in FW (log<sub>2</sub>FC=3.3) and hypomethylated at the promoter and gene body levels. We also identified in the category ‘cytokine receptor activity’ the gene encoding for prolactin receptor (*prlr*), being upregulated in

FW and hypomethylated at the promoter and gene body levels (Table 1). Finally, among the 28% of common GO terms with enriched DMRs and DEGs in the ‘cellular component’ category (Fig. 7C), we observed those associated with ‘bicellular tight junction’ and ‘outer membrane’. Numerous genes encoding for tight junction proteins and claudins appeared as being mainly upregulated in FW and hypomethylated at the promoter level (detailed below).

Interestingly, two genes encoding for DNA methyltransferase 3a (*dnmt3a*) were both downregulated in FW and showed differential methylation patterns (Table 1). One gene was hypomethylated and the other was hypermethylated at the level of the gene body. Methylcytosine dioxygenase 3 (*tet3*), a DNA demethylase, was downregulated in FW.

### 3.6 Freshwater-triggered gene expression changes associated with hyper- and hypomethylation

The distribution of differentially methylated and expressed genes was examined in different genomic contexts (Fig. 8). There was a balanced distribution between upregulated and downregulated genes in FW, ranging from 46-58 % for upregulation and 42-54 % for downregulation when considering hypomethylated genes (exons and introns) and promoters (Fig. 8A). In contrast, in the context of hypermethylation, 62-81 % of the genes and promoters were downregulated and only 19 to 38 % were upregulated (Fig. 8B). It is worth noting that in the first introns, we found the highest proportion (81 %) of downregulated genes in the context of hypermethylation.

KEGG pathway analysis was performed to show the functional enrichment of DEGs and DMGs (Fig. 9 and Table 1, Table 7S). We focused on differentially methylated genes at promoters, first exons or first introns and their expression changes upon salinity transfer. Some pathways involved in ‘regulation of actin cytoskeleton’, ‘focal adhesion’, and ‘calcium signaling pathway’ were statistically enriched for both DEGs and DMGs. Genes encoding for functions related to these pathways had their expression repressed and displayed either a hypermethylation or a hypomethylation in FW (Fig. 9). Regarding the ‘calcium signaling pathway’ category, we identified genes encoding for the SERCA (Sarco Endoplasmic Reticulum Calcium ATPase) pump (*atp2a2*) and several voltage-dependent calcium channels. In several KEGG categories, we identified tropomyosin (*tpm1*) as being hypermethylated and downregulated, as well as genes involved in and in ‘integrin signaling’ (*itga 1, 4, 5, 9*).

The ‘tight junction’ category was enriched, as in the previous analysis, and showed genes that were mainly hypomethylated and upregulated in FW vs SW or hypomethylated and downregulated in FW vs SW (Fig. 9). Ten genes encoding for Claudins were differently expressed and were enriched in DMRs (Table 1). Among them, eight were upregulated in FW and hypomethylated, mainly at promoter level. In this category, we also identified one paralog of tight-junction protein 2 (*tjp2*), the cytoskeleton-associated cingulin-like protein (*cgn*), MarvelD3, a transmembrane component of tight junctions, and the junctional adhesion molecule a-like (*f11r*). These genes were all hypomethylated and upregulated.

The ‘focal adhesion pathway’ was enriched in downregulated genes that were either hyper- or hypomethylated. As indicated previously, we identified several genes involved in integrin signaling with some of them being also hypomethylated (*itga 3, 6, 7*) and a transcription factor, focal adhesion kinase (*ptk2*), that was downregulated and hypomethylated. The pathway ‘regulation of actin cytoskeleton’ was significantly enriched with mainly downregulated genes that were either hyper- or hypomethylated in FW, as indicated previously. Regarding metabolism, the KEGG pathways ‘glycosphingolipid biosynthesis’ and ‘glycerophospholipid metabolism’ and ‘sphingolipid signaling pathway’ were also enriched for DEGs and DMRs (Table 7S).

In the ‘mineral absorption’ pathway, only two genes were highlighted, including one gene encoding for chloride channel 2 (*clcn2*, one of the two paralogs) and one encoding for the copper transporter *ctr1* (*slc31a1*). Both genes appeared hypermethylated and upregulated in FW. We also noticed the upregulation of the prolactin signaling pathway with genes enriched for hypomethylation, as the prolactin receptor (*prlr*) (Table 7S).

## 4. Discussion

The study of DNA methylation dynamics and its contribution to salinity acclimation through changes in gene expression are of particular importance in European sea bass, a truly euryhaline species, that encounters frequent salinity fluctuations in its natural environment. There is clear evidence that a two-week freshwater transfer affects genome-wide DNA methylation in European sea bass juveniles. Salinity-induced methylation changes were compared in different genomic contexts (promoters *vs* the body of genes).

#### 4.1 Gene expression and DNA methylation are inversely correlated in promoters, first exons and first introns

First, we determined if there is a correlation between gene expression and DNA methylation levels in different genomic regions using gill homogenates from the same individuals for both analyses. In *D. labrax*, we observed a global DNA methylation all over the genome, with a depletion at the promoters and transcription start sites. This is consistent with previous observations in vertebrates (Aliaga et al., 2019; Suzuki and Bird, 2008). An inverse correlation between gene expression and DNA methylation levels was found in promoters, first introns and first exons. This inverse correlation has previously been highlighted by Anastasiadi et al. (2018) who compared DNA methylation levels in muscles and testes of *D. labrax*, and later by Liu et al. (2022) in *Anguilla anguilla* muscles for first exons. The presence of unmethylated CpG islands in the proximity of the TSS is consistent with the role of first introns and first exons in the regulation of gene expression. Additionally to promoters, first introns and first exons could thus be involved in transcriptional regulation as highlighted for first introns in humans (Li et al., 2012). We showed that the rest of the introns and exons were highly methylated (>75 %) and did not show any correlation with gene expression, as previously observed in previous studies (Anastasiadi et al., 2018).

#### 4.2 Freshwater transfer overall induces DNA hypomethylation in *D. labrax* gills

Studies on the effect of salinity on DNA methylation dynamics has been performed in plants (Rajkumar et al., 2019; Skorupa et al., 2021) and also in animals, but only in few teleost species (Artemov et al., 2017; Metzger and Schulte, 2018; Heckwolf et al., 2020; Zhang et al., 2022; Yang et al., 2023).

Our data showed that a freshwater transfer in fish gills overall induced hypomethylation of DNA across all chromosomes. Parallely, a downregulation of the expression of two paralogs of DNA methyltransferase 3a was observed, which is consistent with this overall decrease in DNA methylation. Predominant DNA hypomethylation in fresh water *vs* seawater was observed in exons as well as in introns and all over the genome, where DMRs were detected. A salinity effect on DNA methylation level was also observed in threespine stickleback (*G. aculeatus*) of a marine ecotype, where overall hypomethylation was observed in whole fish that were reared for 1 month at high salinity relative to those reared at low salinity (Metzger and Schulte, 2018), which is an inverse tendency than what we observed in *D. labrax* gills. It therefore seems that a medium-term (2 weeks in this study) as well as a long term salinity acclimation (1 month) can affect DNA methylation dynamics in fish tissues. In sea bass, the distribution of DMRs across genomic features (e.g., promoters, exons, introns and intergenic regions) did not differ from the relative proportions of these features in the genome (Tine et al., 2014) which means that fresh water induces methylation changes in all genomic features without targeting specific regions in the genome. Global hypomethylation has previously been shown following several stressors such as metal stress in zebrafish embryos (Bian and Gao., 2021), and salinity stress in the crustacean *Daphnia magna* (Jeremias et al., 2018). Global hypomethylation could be considered as a global response to a stressor, potentially playing a role in the modulation of transcription activity.

#### 4.3 Hypermethylation triggered by freshwater transfer overall induces downregulation of genes

Despite an overall DNA hypomethylation in the sea bass genome, we observed an interesting trend for hypermethylated genes to be silenced at a very high percentage, notably in first introns. When considering genes that were hypermethylated in first introns and show differential expression between salinities, 81% of the genes were downregulated, and only 19% were upregulated, which is intriguing. Genes that were downregulated and hypermethylated in promoters, first exons or first introns belonged to different KEGG categories (Table 7S). Among those, we identified several genes involved in cell-cell adhesion and regulation

of actin cytoskeleton as tropomyosin and a change in integrin turnover. It is known that integrins assembling to the cytoskeleton is important in cell-cell adhesion (Delon and Brown., 2007). There is in fact an extensive remodeling of gills in euryhaline teleosts following salinity transfer, that involves cell proliferation and turnover pathways, leading to epithelial remodeling. In *D. labrax* as in other species, the density and subtypes of gill ionocytes is increased in the freshwater environment (Masroor et al., 2018). We identified several genes involved in the calcium signaling pathway. Calcium is an ubiquitous second messenger regulating numerous cellular processes, including proliferation, cellular metabolism, and cell death. In mammal studies linked to cancer research, the SERCA pump (encoded by *atp2a*), which sequesters  $\text{Ca}^{2+}$  into the endoplasmic reticulum (ER), as well as other calcium regulated genes, showed altered expression patterns that coincided with increased promoter methylation (Bertocci et al., 2022). In *D. labrax*, the hypermethylation of the gene encoding for SERCA might contribute to its significantly lower expression in FW (log2FC: -0,38), which could lead to increased cytoplasmic calcium availability. We did not measure any expression difference in plasma membrane  $\text{Ca}^{2+}$  ATPase (*pmca*) between salinity conditions, which is an important pump expressed in gill ionocytes to take up  $\text{Ca}^{2+}$  from FW environments.

#### 4.4 Freshwater transfer affects DNA methylation in crucial genes involved in maintaining hydromineral balance

We showed that a freshwater transfer affects expression changes in genes that were differentially methylated, which suggests that a change in salinity could induce an altered pattern of DNA methylation, which in turn could have functional consequences and allow sea bass to display phenotypic variation through gene expression changes linked to hydromineral balance.

Gene expression changes in fish gills following a salinity change have been shown in numerous species (Leguen et al., 2015; Qin et al., 2022) whereas studies on DNA methylation changes in different salinity conditions are scarce. We focused in this study on genes that are involved in osmoregulation, cell volume regulation and acid base regulation and that display gene expression as well as DNA methylation changes (Table 1). Among them, the gene encoding for water channel Aquaporin 3 (*aqp3*) is highly induced in FW vs SW (log2FC=3.3), and hypomethylated at promoter and gene body levels. This gene is expressed in ionocytes and is known to be overexpressed in gills of numerous species in FW, notably for the basolateral release of water from ionocytes to the serosal fluid to prevent cell swelling (Cutler and Cramb., 2002; Giffard-Mena et al., 2007). In studies on mammal gastric carcinoma, *aqp3* was shown to be hypermethylated at its promoter and first exon, which limited its expression (Wang et al., 2019). In fish, *aqp3* gene expression is controlled by cortisol and prolactin, where prolactin induces its expression and cortisol decreases its expression in gills of Mozambique tilapia *Oreochromis mossambicus* (Breves et al., 2016). Interestingly, in *D. labrax*, the gene *nr3c1* encoding for the glucocorticoid receptor was repressed and hypomethylated at its gene body (GB). Moreover, the *prlra* gene encoding for one of the two prolactin receptor paralogs was upregulated in FW vs SW (log2FC=1.93) as shown previously (L'Honore et al. 2020) and hypomethylated at promoter and GB levels. This is consistent with the observed upregulation and hypomethylation (at promoters, first exons or introns) of the 'prolactin signaling pathway'. DNA methylation changes of genes encoding for hormone receptors could be key regulators of osmoregulatory processes. To our knowledge, no data are available on the effect of methylation changes on *prlr* expression in fish. However, studies on KO mice brains with selective disruption of the dopamine D2 receptor in neurons, have shown an upregulation of *prlr* correlated with decreased methylation of their promoters (Brie et al., 2020).

Regarding ion channels and transporters that are involved in salt uptake, we identified chloride channels *clcn2* and *clcn3* that were upregulated in FW vs SW (with log2FC of 2.63 and 0.71 respectively). *clcn2* was hypermethylated at GB level. Interestingly we found another paralog of *clcn2*, that was downregulated in FW (log2FC=-2.13) and hypomethylated in GB. Both Clcn2 and Clcn3 channels have been localized in basolateral membranes of ionocytes and are suspected to transport  $\text{Cl}^-$  to the blood for its uptake (Tang et al., 2010; Bossus et al., 2013). *clcn2* expression and protein changes according to salinity have been shown in several studies, although with sometimes contrasting data (Root et al., 2021; Bossus et al., 2013) that might be linked to the presence of two *clcn2* paralogs that were not differentiated. Several genes encode

for  $\text{Na}^+/\text{K}^+$ -ATPase, which is a key active ion transporting pump expressed in basolateral membranes of gill ionocytes. As expected, the major paralog (*atp1a1a*) encoding for subunit  $\text{NKA}\alpha 1$  was upregulated in FW vs SW as shown previously by Blondeau-Bidet et al. (2019) in *D. labrax* gills. We also observed a hypomethylation at promoter and GB levels. *atp1a3* (encoding for the  $\text{NKA}\alpha 3$  subunit), which has not been investigated so far in *D. labrax* gills, was also upregulated and hypomethylated in promoters. In *D. labrax* SW-type ionocytes, the apical chloride channel CFTR and basolateral cotransporter NKCC1 are crucial proteins involved in salt secretion (Lorin-Nebel et al. 2006; Bodinier et al., 2009). Both genes encoding for these proteins were downregulated in FW and hypermethylated at GB level. Fougere et al. (2020) showed that focal adhesion kinases are, according to their phosphorylation state, colocalized with apical tight junctions and CFTR in apical membranes of ionocytes of *Fundulus heteroclitus*, and are involved in ion secretion by these cells. We identified two *ptk2* genes encoding for focal adhesion kinase 1 which were downregulated ( $\log_2\text{FC} = -0.4113$  and  $-0.7749$ ) and hypomethylated (GB and promoters) but the functional link between Ptk2 with apically localized proteins in ionocytes remains to be shown in *D. labrax*. V-type  $\text{H}^+$  ATPase (VHA) is another important pump expressed in fish gill ionocytes. It is involved in  $\text{H}^+$  secretion (for acid-base balance) coupled to transepithelial  $\text{Na}^+$  uptake (for osmoregulation). We identified three genes encoding for VHA that showed expression and methylation changes upon FW transfer (Table 1). Together, all these data point to significant methylation changes in key genes involved in hyper- and hypo-osmoregulation as well as acid-base regulation. This is consistent with the statement that salinity affects the plastic responses through DNA methylation changes, to maintain hydromineral balance, as already mentioned in other species (Heckwolf et al. 2020).

#### 4.5 Paracellular permeability-related genes are hypomethylated and upregulated

In clinical studies on mammal cancer where disruption of cell-cell junctions is frequently found, investigations have shown a link between claudin overexpression and DNA hypomethylation for several claudins (Li et al., 2018), including *cldn4* (Kwon et al., 2011). In fish gills, the tightening of the gill epithelium is a natural and essential process in fresh water in order to avoid excess water entry and limit passive ion loss. Euryhaline species have to constantly adjust gill permeability through the expression of tight or leaky junctions. A striking result of this study is the consistent promoter hypomethylation and upregulation of genes involved in paracellular permeability and the formation of tight junctions. In both analyses (KEGG pathway and GO-term enrichment analyses), tight junctions appeared among the most significant pathways. In sticklebacks, Metzger and Schulte (2018) also showed that the category cell-cell-junction appeared among the top ten enriched cellular component GO categories comparing differentially methylated cytosines in different salinity conditions, which highly suggests that methylation changes control the expression of these genes in fish. In another study comparing slow-twitch and fast-twitch muscles in the teleost *Pseudocaranx dentex*, Li et al. (2022) also identified a correlation between DNA methylation and gene expression levels in genes involved in cell junctions (tight and adherens junctions). Tight junctions are composed of multiple membrane-spanning proteins such as occludins, claudins and several junctional adhesion molecules (Chasiotis et al., 2012). Claudins are very diverse in fish and mammals (Engelund et al., 2012) with a total of 61 *cldn* genes in European sea bass including all paralogs. Among the different genes that show differential expression and methylation levels, *cldn4* and *cldn8* are supposed to be involved in increasing the epithelial tightness (Bagherie-Lachidan et al., 2009) which is essential in freshwater environments. We found two genes encoding for Claudin 8 with a significant upregulation ( $\log_2\text{FC}$ : 1.44 and 0.68) and hypomethylation. In gills of puffer fish (*Tetraodon nigroviridis*), one *claudin 8* paralog (*Tncldn8d*) also showed an increased expression in FW, but not the 3 others (Bagherie-Lachidan et al., 2009). The overexpression of *cldn 4* in FW was shown in other teleost species, like tilapia (*Oreochromis mossambicus*) (Tipsmark et al., 2008), killifish (Whitehead et al., 2012), and rainbow trout (*Oncorhynchus mykiss*) (Leguen et al., 2015). We identified two genes encoding for *D. labrax* Claudin 4 paralogs that were both upregulated in FW ( $\log_2\text{FC}$ : 0.87 and 1.47) and hypomethylated in promoters as well as other key genes involved in tight junction assembling (*egn*, *f11r*, *marveld3*). Given the enrichment of the tight junction pathway for upregulation and hypomethylation, there is some evidence that claudin promoters, first exons or introns are a preferential target for differential methylation in changing salinity environments in euryhaline *D. labrax*. Studies in other teleost species on

the effect of methylation on the tight junction pathway are required to confirm this trend in fish.

#### 4.6 Metabolism and salinity acclimation

Our analyses showed changes in the expression and methylation of genes involved in lipid, protein and carbohydrate metabolism as well as mitochondrial functions. The transition from a seawater- to a freshwater physiology requires gill epithelium turnover and active ion transport and is thus an energy consuming process. This energy is provided by metabolites related to carbohydrates, proteins/amino acids and lipids, transported from liver stores to the blood, towards the gill. In addition to energy sources provided by the blood, there is also a local energy supply at the gill level necessary for the modulation and stimulation of gill epithelium reorganization and ion transport mechanisms (Hwang and Lee., 2007).

Lipid metabolism in fish gills has been widely overlooked, despite the growing number of studies in mammals indicating the importance of lipids in ion channel regulation notably through lipid-protein interactions (Rosenhouse-Dantsker et al., 2012). In both analyses (GO-term and KEGG enrichment analyses), the sphingolipid synthesis and signaling pathways were significantly enriched and are thus worth considering. Sphingolipids are involved in multiple functions, such as immune-related functions, cellular growth, differentiation, apoptosis and have been argued to have second-messenger functions (Shayman, 2000). Sphingolipids and mainly sphingomyelin, are also major components of membrane microdomains, called lipid rafts, where they are involved in the regulation of ion channels (Rosenhouse-Dantsker et al., 2012). Lipid raft abundance in fish gills can in fact change upon salinity transfer. They can be enriched in membrane transporters like  $\text{Na}^+/\text{K}^+$ -ATPase, as shown in tilapia *O. mossambicus* and milkfish *Chanos chanos* gills (Lin et al., 2021). Hydrolysis of sphingomyelin due to a cell stress can lead to ceramide formation, which is implicated in numerous physiological functions. Several ion channels such as CFTR (Ramu et al., 2007) and voltage gated  $\text{K}^+$  channels (Fan et al., 1997) have been shown to be inhibited by ceramide. In this study, *sphingomyelin synthase (sgms1)* was upregulated and hypomethylated in FW. We also observed a downregulation of *serine palmitoyltransferase (spltc2)* which is involved in the first step of sphingolipid biosynthesis (Hanada., 2003) and *ceramide synthase 5 (cers5)*. Altogether, these results indicate a potential change in the ceramide species profiles (Gault et al., 2010). However, the potential functional link between methylation changes and expression changes of genes involved in sphingolipid metabolism is not clear and needs further investigation.

Studies have pointed out that the enzymes involved in methylation and demethylation have substrates that are responsive to cellular metabolism (Reid et al., 2017). Mitochondria provide key metabolites for epigenetic processes (Shaughnessy et al., 2014). The availability of these metabolites change, when fish are energetically challenged by environmental stressors. For DNA methyltransferases, substrates and cofactors include methylthioadenosine (MTA), S-adenosylmethionine (SAM) and S-adenosylhomocysteine (SAH) for example whereas for DNA demethylases (TET-family), other metabolites are used as succinate, fumarate, ... being intermediates of the TCA cycle (Reid et al., 2017). We observed changes in the expression of genes linked to methionine metabolism (*ahcyl1, 2, mtap*) and an overall overexpression of genes involved in the TCA cycle (*dlst, sdha, sdhd, sdhb, cs*). This clearly displays changes in metabolic pathways and energetic status, which could directly affect the epigenome and DNA methylation dynamics. In gills of sea bass transferred to FW, ionocytes, previously called mitochondria-rich cells due to their high abundance of mitochondria, are present at higher densities with higher energy-consuming  $\text{Na}^+/\text{K}^+$ -ATPase activities (Masroor et al., 2018). We also measured higher expression of paralogs encoding for the  $\text{V-H}^+$ -ATPase indicating a high energy demand for transepithelial ion transport in FW. In accordance with this, we observed higher mitochondrial activities in FW. Mitochondria have a central role in energy (ATP) production but also in metabolite production in the TCA cycle and mitochondria-nuclear signaling. These processes can be linked to epigenetic regulation. As chromatin-modifying enzymes use as substrates and cofactors metabolites derived from diverse metabolic pathways including notably the TCA cycle (Lopes, 2020), salinity-driven changes in transcription of these genes might also directly affect the availability of substrates for chromatin-modifying enzymes and affect DNA methylation dynamics. Relationships between genes, environment and epigenetic marks, and the variation of those marks still require more investigations to gather a full understanding of the determinism of salinity acclimation in fish.

## 5. Conclusion

We have investigated salinity-induced DNA methylation and its role in plasticity and gene expression in gills of euryhaline European sea bass. This study highlighted that genes with low methylation levels in first exons, first introns and promoters are generally highly expressed. We also showed that fresh water triggers an overall hypomethylation of the genome. Our investigation showed that pathways involved in tight junctions are highly enriched in upregulated genes displaying hypomethylated promoters. We also identified other pathways as lipid metabolism, calcium signaling and regulation of actin cytoskeleton that were enriched for gene expression and DNA methylation changes in either promoters or first exons/introns. Numerous key genes involved in transepithelial ion transport of gill ionocytes also show methylation and gene expression changes. Interestingly, mitochondria metabolism is strongly activated, suggesting a modulation of metabolite availability as substrate for chromatin-modifying enzymes. We recommend further investigation of methylation dynamics in environmentally challenged fish in order to determine the role of methylation changes in phenotypic plasticity, acclimation and adaptation.

## Acknowledgments

We thank the technicians of the Ifremer Palavas-les-flots Research Station for their help in maintaining sea bass. We also thank Céline Reisser for her advise on DNA methylome and transcriptome analysis. This work was conducted with the support of LabEx CeMEB, an ANR « Investissements d’avenir » program (ANR-10-LABX-04-01), funded through the I-SITE Excellence Program of the University of Montpellier, under the Investissements France 2030.

## Conflict of Interest

The authors have no conflicts of interest to declare.

## Author Contributions

EBB : data curation, formal analysis, investigation, methodology, visualization, writing -original draft ; CC : conceptualization, funding acquisition, writing-review&editing ; CLN : conceptualization, funding acquisition, project administration, resources, supervision, writing -original draft ; EF : conceptualization, writing-review&editing ; GB : investigation ; TLH : investigation.

## References

- Akalin, A., Kormaksson, M., Li, S., Garrett-Bakelman, F. E., Figueroa, M. E., Melnick, A., & Mason, C. E. (2012). methylKit: a comprehensive R package for the analysis of genome-wide DNA methylation profiles. *Genome Biology*, *13*(10), R87. <https://doi.org/10.1186/gb-2012-13-10-r87>
- Aliaga, B., Bulla, I., Mouahid, G., Duval, D., & Grunau, C. (2019). Universality of the DNA methylation codes in Eucaryotes. *Scientific Reports*, *9*(1), 1–11. <https://doi.org/10.1038/s41598-018-37407-8>
- Anastasiadi, D., Díaz, N., & Piferrer, F. (2017). Small ocean temperature increases elicit stage-dependent changes in DNA methylation and gene expression in a fish, the European sea bass. *Scientific Reports*, *7*(1), 12401. <https://doi.org/10.1038/s41598-017-10861-6>
- Anastasiadi, D., Esteve-Codina, A., & Piferrer, F. (2018). Consistent inverse correlation between DNA methylation of the first intron and gene expression across tissues and species. *Epigenetics and Chromatin*, *11*(1). <https://doi.org/10.1186/s13072-018-0205-1>
- Anders, S., & Huber, W. (2010). Differential expression analysis for sequence count data. *Genome Biology*, *11*(10), R106. <https://doi.org/10.1186/gb-2010-11-10-r106>
- Andrews, S. (2010). *FastQC-A Quality Control application for FastQ files*. Artemov, A. v., Mugue, N. S., Rastorguev, S. M., Zhenilo, S., Mazur, A. M., Tsygankova, S. v., Boulygina, E. S., Kaplun, D., Nedoluzhko, A. v., Medvedeva, Y. A., & Prokhortchouk, E. B. (2017). Genome-wide DNA methylation profiling reveals epigenetic adaptation of stickleback to marine and freshwater conditions. *Molecular Biology and Evolution*, *34*(9), 2203–2213. <https://doi.org/10.1093/molbev/msx156>
- Bagherie-Lachidan, M., Wright, S. I., & Kelly, S. P. (2009). Claudin-8 and -27 tight junction proteins in puffer fish *Tetraodon nigroviridis* acclimated to freshwater and seawater. *Journal of Comparative Physiology B*, *179*(4), 419–431. <https://doi.org/10.1007/s00360-008-0326-0>
- Bertocci, L. A., Rovatti, J. R., Wu, A.,

Morey, A., Bose, D. D., & Kinney, S. R. M. (2022). Calcium handling genes are regulated by promoter DNA methylation in colorectal cancer cells. *European Journal of Pharmacology*, 915, 174698. <https://doi.org/10.1016/j.ejphar.2021.174698>

Brie, B., Ornstein, A., Ramirez, M.C., Lacau-Mengido, I., Becu-Villalobos, D. (2020). Epigenetic modifications in the GH-dependent Prlr, Hnf6, Cyp7b1, Adh1 and Cyp2a4 genes. *J. Molecular Endocrinology*, 64(3), 165-179. <https://doi.org/10.1530/JME-19-0205>

Bian, X., & Gao, Y. (2021). DNA methylation and gene expression alterations in zebrafish embryos exposed to cadmium. *Environmental Science and Pollution Research*, 28(23), 30101–30110. <https://doi.org/10.1007/s11356-021-12691-6>

Bird, A. (2002). DNA methylation patterns and epigenetic memory. In *Genes and Development* (Vol. 16, Issue 1, pp. 6–21). <https://doi.org/10.1101/gad.947102>

Blondeau-Bidet, E., Hiroi, J., & Lorin-Nebel, C. (2019). Ion uptake pathways in European sea bass *Dicentrarchus labrax*. *Gene*, 692, 126–137. <https://doi.org/10.1016/j.gene.2019.01.006>

Bodinier, C., Lorin-Nebel, C., Charmantier, G., Boulo, V. (2009). Influence of salinity on the localization and expression of the CFTR chloride channel in the ionocytes of juvenile *Dicentrarchus labrax* exposed to seawater and freshwater. *Comparative Biochemistry and Physiology A*, 153(3), 345-351. <https://doi.org/10.1016/j.cbpa.2009.03.011>

Bossus, M., Charmantier, G., Blondeau-Bidet, E., Valletta, B., Boulo, V., & Lorin-Nebel, C. (2013). The ClC-3 chloride channel and osmoregulation in the European Sea Bass, *Dicentrarchus labrax*. *Journal of Comparative Physiology B: Biochemical, Systemic, and Environmental Physiology*, 183(5), 641–662. <https://doi.org/10.1007/s00360-012-0737-9>

Brenet, F., Moh, M., Funk, P., Feierstein, E., Viale, A. J., Socci, N. D., & Scandura, J. M. (2011). DNA Methylation of the First Exon Is Tightly Linked to Transcriptional Silencing. *PLoS ONE*, 6(1), e14524. <https://doi.org/10.1371/journal.pone.0014524>

Breves, J. P., Inokuchi, M., Yamaguchi, Y., Seale, A. P., Hunt, B. L., Watanabe, S., Lerner, D. T., Kaneko, T., & Grau, E. G. (2016). Hormonal regulation of aquaporin 3: opposing actions of prolactin and cortisol in tilapia gill. *Journal of Endocrinology*, 230(3), 325–337. <https://doi.org/10.1530/JOE-16-0162>

Chang, C.-H., Liu, C.-J., Lu, W.-J., Wu, L.-Y., Lai, K.-J., Lin, Y.-T., & Lee, T.-H. (2022). Hypothermal Effects on Energy Supply for Ionocytes in Gills of Freshwater- and Seawater-Acclimated Milkfish, *Chanos chanos*. *Frontiers in Marine Science*, 9. <https://doi.org/10.3389/fmars.2022.880103>

Chang, J. C.-H., Wu, S.-M., Tseng, Y.-C., Lee, Y.-C., Baba, O., & Hwang, P.-P. (2007). Regulation of glycogen metabolism in gills and liver of the euryhaline tilapia (*Oreochromis mossambicus*) during acclimation to seawater. *Journal of Experimental Biology*, 210(19), 3494–3504. <https://doi.org/10.1242/jeb.007146>

Chasiotis, H., Kolosov, D., Bui, P., & Kelly, S. P. (2012). Tight junctions, tight junction proteins and paracellular permeability across the gill epithelium of fishes: A review. In *Respiratory Physiology and Neurobiology* (Vol. 184, Issue 3, pp. 269–281). <https://doi.org/10.1016/j.resp.2012.05.020>

Cutler, C. P., & Cramb, G. (2002). Branchial expression of an aquaporin 3 (AQP-3) homologue is downregulated in the European eel *Anguilla anguilla* following seawater acclimation. *Journal of Experimental Biology*, 205(17), 2643–2651. <https://doi.org/10.1242/jeb.205.17.2643>

Czubak-Prowizor, K., Babinska, A., & Swiatkowska, M. (2022). The F11 Receptor (F11R)/Junctional Adhesion Molecule-A (JAM-A) (F11R/JAM-A) in cancer progression. *Molecular and Cellular Biochemistry*, 477(1), 79–98. <https://doi.org/10.1007/s11010-021-04259-2>

De Larco, J. E., Wuertz, B. R. K., Yee, D., Rickert, B. L., & Furcht, L. T. (2003). Atypical methylation of the interleukin-8 gene correlates strongly with the metastatic potential of breast carcinoma cells. *Proceedings of the National Academy of Sciences of the United States of America*, 100(24), 13988–13993. <https://doi.org/10.1073/pnas.2335921100>

Delon, I., & Brown, N. H. (2007). Integrins and the actin cytoskeleton. *Current Opinion in Cell Biology*, 19(1), 43–50. <https://doi.org/10.1016/j.ceb.2006.12.013>

Dobin, A., & Gingeras, T. R. (2016). Optimizing RNA-seq mapping with STAR. In *Methods in Molecular Biology* (Vol. 1415, pp. 245–262). Humana Press Inc. [https://doi.org/10.1007/978-1-4939-3572-7\\_13](https://doi.org/10.1007/978-1-4939-3572-7_13)

Dufour, V., Cantou, M., & Lecomte, F. (2009). Identification of sea bass (*Dicentrarchus labrax*) nursery areas in the north-western Mediterranean Sea. *Journal of the Marine Biological Association of the United Kingdom*, 89(7), 1367–1374. <https://doi.org/10.1017/S0025315409000368>

Engelund, M. B., Yu, A. S. L., Li, J., Madsen, S. S., Færgeman, N. J., & Tipsmark, C. K. (2012). Functional characterization and localization of a gill-specific claudin isoform in Atlantic salmon. *American Journal of Physiology-Regulatory, Integrative and Comparative Physiology*, 302(2), R300–R311. <https://doi.org/10.1152/ajpregu.00286.2011>

Ewels, P., Magnusson, M., Lundin, S., & Käller, M. (2016). MultiQC: summarize analysis results for multiple tools and samples in a single report. *Bioinformatics*, 32(19), 3047–3048. <https://doi.org/10.1093/bioinformatics/btw354>

Z., & Makielski, J. C. (1997). Anionic Phospholipids Activate ATP-sensitive Potassium Channels. *Journal of Biological Chemistry*, 272(9), 5388–5395. <https://doi.org/10.1074/jbc.272.9.5388> Feng, S., Cokus, S. J., Zhang, X., Chen, P. Y., Bostick, M., Goll, M. G., Hetzel, J., Jain, J., Strauss, S. H., Halpern, M. E., Ukomadu, C., Sadler, K. C., Pradhan, S., Pellegrini, M., & Jacobsen, S. E. (2010). Conservation and divergence of methylation patterning in plants and animals. *Proceedings of the National Academy of Sciences of the United States of America*, 107(19), 8689–8694. <https://doi.org/10.1073/pnas.1002720107> Flores, K. B., Wolschin, F., & Amdam, G. v. (2013). The role of methylation of DNA in environmental adaptation. *Integrative and Comparative Biology*, 53(2), 359–372. <https://doi.org/10.1093/icb/ict019> Fougere, B., Barnes, K.R., Francis, M.E., Claus, L.N., Cozzi, R.R.F., Marshall, W.S. (2020). Focal adhesion kinase and osmotic responses in ionocytes of *Fundulus heteroclitus*, a euryhaline teleost fish. *Comparative Biochemistry and Physiology A: Molecular & Integrative Physiology* 241:110639. <https://doi.org/10.1016/j.cbpa.2019.110639> Gault, C. R., Obeid, L. M., & Hannun, Y. A. (2010). *An Overview of Sphingolipid Metabolism: From Synthesis to Breakdown* (pp. 1–23). [https://doi.org/10.1007/978-1-4419-6741-1\\_1](https://doi.org/10.1007/978-1-4419-6741-1_1) Giffard-Mena, I., Boulo, V., Aujoulat, F., Fowden, H., Castille, R., Charmantier, G., & Cramb, G. (2007). Aquaporin molecular characterization in the sea-bass (*Dicentrarchus labrax*): The effect of salinity on AQP1 and AQP3 expression. *Comparative Biochemistry and Physiology Part A: Molecular & Integrative Physiology*, 148(2), 430–444. <https://doi.org/10.1016/j.cbpa.2007.06.002> Hanada, K. (2003). Serine palmitoyltransferase, a key enzyme of sphingolipid metabolism. *Biochimica et Biophysica Acta (BBA) - Molecular and Cell Biology of Lipids*, 1632(1–3), 16–30. [https://doi.org/10.1016/S1388-1981\(03\)00059-3](https://doi.org/10.1016/S1388-1981(03)00059-3) Heckwolf, M. J., Meyer, B. S., Häslner, R., Höppner, M. P., Eizaguirre, C., & Reusch, T. B. H. (2020). Two different epigenetic information channels in wild three-spined sticklebacks are involved in salinity adaptation. *Science Advances*, 6(12). <https://doi.org/10.1126/sciadv.aaz1138> Hwang, P. P., & Lee, T. H. (2007). New insights into fish ion regulation and mitochondrion-rich cells. In *Comparative Biochemistry and Physiology - A Molecular and Integrative Physiology* (Vol. 148, Issue 3, pp. 479–497). Elsevier Inc. <https://doi.org/10.1016/j.cbpa.2007.06.416> Jeremias, G., Barbosa, J., Marques, S.M., De Schampelaere, K.A.C., Van Nieuwerburgh, F., Deforce, D., Gonçalves, F.J.M., Pereira, J.L., & Asselman, J. (2018). Transgenerational inheritance of DNA hypomethylation in *Daphnia magna* in response to salinity stress. *Environmental Science & Technology*, 52(17), 10114–10123. DOI: 10.1021/acs.est.8b03225 Jones, P. A. (2012). Functions of DNA methylation: islands, start sites, gene bodies and beyond. *Nature Reviews Genetics*, 13(7), 484–492. <https://doi.org/10.1038/nrg3230> Korthauer, K. (2017). Detection and inference of differentially methylated regions from bisulfite sequencing Differential methylation commonly studied in. Krueger, F. (2012). Trim Galore: a wrapper tool around Cutadapt and FastQC to consistently apply quality and adapter trimming to FastQ files, with some extra functionality for MspI-digested RRBS-type (Reduced Representation Bisulfite-Seq) libraries. [URL Http://Www. Bioinformatics. Babraham. Ac. Uk/Projects/Trim\\_galore/.](http://www.bioinformatics.babraham.ac.uk/projects/Trim_galore/) (Date of Access: 28/04/2016). Krueger, F., & Andrews, S. R. (2011). Bismark: A flexible aligner and methylation caller for Bisulfite-Seq applications. *Bioinformatics*, 27(11), 1571–1572. <https://doi.org/10.1093/bioinformatics/btr167> Kwon, M.J., Kim, S.H., Jeong, H.M., Jung, H.S., Kim, S.S., Lee, J.E., Gye, M.C., Erkin, O.C., Koh, S.S., Choi, Y.L., Park, C.K., & Shin, Y.K. (2011). Claudin-4 overexpression is associated with epigenetic derepression in gastric carcinoma. *Lab Invest*. 91(11):1652-67. doi: 10.1038/labinvest.2011.117. Larsen, F., Gundersen, G., Lopez, R., & Prydz, H. (1992). CpG islands as gene markers in the human genome. *Genomics*, 13(4), 1095–1107. [https://doi.org/10.1016/0888-7543\(92\)90024-M](https://doi.org/10.1016/0888-7543(92)90024-M) Leguen, I., le Cam, A., Montfort, J., Peron, S., & Fautrel, A. (2015). Transcriptomic analysis of trout gill ionocytes in fresh water and sea water using laser capture microdissection combined with microarray analysis. *PLoS ONE*, 10(10). <https://doi.org/10.1371/journal.pone.0139938> L'Honoré, T., Farcy, E., Blondeau-Bidet, E., & Lorin-Nebel, C. (2020). Inter-individual variability in freshwater tolerance is related to transcript level differences in gill and posterior kidney of European sea bass. *Gene*, 741. <https://doi.org/10.1016/j.gene.2020.144547> Liao, Y., Smyth, G. K., & Shi, W. (2014). featureCounts: an efficient general purpose program for assigning sequence reads to genomic features. *Bioinformatics*, 30(7), 923–930. <https://doi.org/10.1093/bioinformatics/btt656> Li, B., Wang, H., Li, A., An, C., Zhu, L., Liu, S., & Zhuang, Z. (2022). The Landscape of DNA Methylation Generates Insight Into Epigenetic Regulation of Differences Between Slow-Twitch and Fast-Twitch Muscles in *Pseudocaranx dentex*. *Frontiers in Marine Science*, 9. <https://doi.org/10.3389/fmars.2022.916373>

Li, H., Chen, D., & Zhang, J. (2012). Analysis of Intron Sequence Features Associated with Transcriptional Regulation in Human Genes. *PLoS ONE*, 7(10), e46784. <https://doi.org/10.1371/journal.pone.0046784>

Li, H.P., Peng, C.C., Wu, C.C., Chen, C.H., Shih, M.J., Huang, M.Y., Lai, Y.R., Chen, Y.L., Chen, T.W., Tang, P., Chang, Y.S., Chang, K.P. & Hsu, C.L. (2018). Inactivation of the tight junction gene *CLDN11* by aberrant hypermethylation modulates tubulins polymerization and promotes cell migration in nasopharyngeal carcinoma. *J. Exp. Clin. Cancer Res.* 37 : 102. <https://doi.org/10.1186/s13046-018-0754-y>

Lin, Y.-T., Hu, Y.-C., Wang, Y.-C., Hsiao, M.-Y., Lorin-Nebel, C., & Lee, T.-H. (2021). Differential expression of two ATPases revealed by lipid raft isolation from gills of euryhaline teleosts with different salinity preferences. *Comparative Biochemistry and Physiology Part B: Biochemistry and Molecular Biology*, 253, 110562. <https://doi.org/10.1016/j.cbpb.2021.110562>

Liu, S., Tengstedt, A. N. B., Jacobsen, M. W., Pujolar, J. M., Jónsson, B., Lobón-Cervia, J., Bernatchez, L., & Hansen, M. M. (2022). Genome-wide methylation in the panmictic European eel (*Anguilla anguilla*). *Molecular Ecology*, 31(16), 4286–4306. <https://doi.org/10.1111/mec.16586>

Lopes, A.F.C. (2020). Mitochondrial metabolism and DNA methylation: a review of the interaction between two genomes. *Clin. Epigenet.* 12, 182 (2020). <https://doi.org/10.1186/s13148-020-00976-5>

Lorin-Nebel C., Boulo V., Bodinier C. & Charmantier G. (2006). The Na<sup>+</sup>/K<sup>+</sup>/2Cl<sup>-</sup> cotransporter in the sea-bass *Dicentrarchus labrax*: Ontogeny and expression according to the salinity. *J. Exp. Biol.* 209: 4908-4922.

Love, M. I., Huber, W., & Anders, S. (2014). Moderated estimation of fold change and dispersion for RNA-seq data with DESeq2. *Genome Biology*, 15(12), 550. <https://doi.org/10.1186/s13059-014-0550-8>

Martin, M. (2011). Cutadapt removes adapter sequences from high-throughput sequencing reads. *EMBnet.Journal*, 17(1), 10. <https://doi.org/10.14806/ej.17.1.200>

Masroor, W., Farcy, E., Gros, R., & Lorin-Nebel, C. (2018). Effect of combined stress (salinity and temperature) in European sea bass *Dicentrarchus labrax* osmoregulatory processes. *Comparative Biochemistry and Physiology Part A: Molecular & Integrative Physiology*, 215, 45–54. <https://doi.org/10.1016/j.cbpa.2017.10.019>

Maunakea, A. K., Nagarajan, R. P., Bilenky, M., Ballinger, T. J., D'Souza, C., Fouse, S. D., Johnson, B. E., Hong, C., Nielsen, C., Zhao, Y., Turecki, G., Delaney, A., Varhol, R., Thiessen, N., Shchors, K., Heine, V. M., Rowitch, D. H., Xing, X., Fiore, C., ... Costello, J. F. (2010). Conserved role of intragenic DNA methylation in regulating alternative promoters. *Nature*, 466(7303), 253–257. <https://doi.org/10.1038/nature09165>

Metzger, D. C. H., & Schulte, P. M. (2016). Epigenomics in marine fishes. *Marine Genomics*, 30, 43–54. <https://doi.org/10.1016/j.margen.2016.01.004>

Metzger, D. C. H., & Schulte, P. M. (2018). The DNA methylation landscape of stickleback reveals patterns of sex chromosome evolution and effects of environmental salinity. *Genome Biology and Evolution*, 10(3), 775–785. <https://doi.org/10.1093/gbe/evy034>

Moran, P., Marco-Rius, F., Megias, M., Covelo-Soto, L., & Perez-Figueroa, A. (2013). Environmental induced methylation changes associated with seawater adaptation in brown trout. *Aquaculture*, 392–395, 77–83. <https://doi.org/10.1016/j.aquaculture.2013.02.006>

Navarro-Martin, L., Vinas, J., Ribas, L., Diaz, N., Gutierrez, A., di Croce, L., & Piferrer, F. (2011). DNA methylation of the gonadal aromatase (*cyp19a*) promoter is involved in temperature-dependent sex ratio shifts in the European sea bass. *PLoS Genetics*, 7(12). <https://doi.org/10.1371/journal.pgen.1002447>

Newell-Price, J., Clark, A. J., & King, P. (2000). DNA methylation and silencing of gene expression. *Trends in Endocrinology and Metabolism: TEM*, 11(4), 142–148. [https://doi.org/10.1016/s1043-2760\(00\)00248-4](https://doi.org/10.1016/s1043-2760(00)00248-4)

Pickett, G. D., Kelley, D. F., & Pawson, M. G. (2004). The patterns of recruitment of sea bass, *Dicentrarchus labrax* L. from nursery areas in England and Wales and implications for fisheries management. *Fisheries Research*, 68(1–3), 329–342. <https://doi.org/10.1016/j.fishres.2003.11.013>

Qin, H., Yu, Z., Zhu, Z., Lin, Y., Xia, J., & Jia, Y. (2022). The integrated analyses of metabolomics and transcriptomics in gill of GIFT tilapia in response to long term salinity challenge. *Aquaculture and Fisheries*, 7(2), 131–139. <https://doi.org/10.1016/J.AAF.2021.02.006>

Quinlan, A. R. (2014). BEDTools: The Swiss-Army Tool for Genome Feature Analysis. *Current Protocols in Bioinformatics*, 47(1), 11.12.1-11.12.34. <https://doi.org/10.1002/0471250953.bi1112s47>

Rajkumar, M. S., Shankar, R., Garg, R., & Jain, M. (2019). Role of DNA methylation dynamics in desiccation and salinity stress responses in rice cultivars. *BioRxiv*, 558064. <https://doi.org/10.1101/558064>

Raleigh, D. R., Marchiando, A. M., Zhang, Y., Shen, L., Sasaki, H., Wang, Y., Long, M., & Turner, J. R. (2010). Tight Junction-associated MARVEL Proteins MarvelD3, Tricellulin, and Occludin Have Distinct but Overlapping Functions. *Molecular Biology of the Cell*, 21(7), 1200–1213. <https://doi.org/10.1091/mbc.e09-08-0734>

Ramirez, F., Ryan, D. P., Gruning, B., Bhardwaj, V., Kilpert, F., Richter, A. S., Heyne, S., Dundar, F., & Manke, T. (2016). deepTools2: a next generation web server for deep-sequencing data analysis. *Nucleic Acids Research*, *44*(W1), W160–W165. <https://doi.org/10.1093/nar/gkw257>

Ramu, Y., Xu, Y., & Lu, Z. (2007). Inhibition of CFTR Cl<sup>-</sup> channel function caused by enzymatic hydrolysis of sphingomyelin. *Proceedings of the National Academy of Sciences*, *104*(15), 6448–6453. <https://doi.org/10.1073/pnas.0701354104>

Reid, M.A., Dai, Z. & Locasale, J.W. (2017). The impact of cellular metabolism on chromatin dynamics and epigenetics. *Nat Cell Biol* *19*, 1298–1306. <https://doi.org/10.1038/ncb3629>

Root, L., Campo, A., MacNiven, L., Con, P., Cnaani, A., & Kultz, D. (2021). Nonlinear effects of environmental salinity on the gill transcriptome versus proteome of *Oreochromis niloticus* modulate epithelial cell turnover. *Genomics*, *113*(5), 3235–3249. <https://doi.org/10.1016/j.ygeno.2021.07.016>

Rosenhouse-Dantsker, A., Mehta, D., & Levitan, I. (2012). Regulation of Ion Channels by Membrane Lipids. In *Comprehensive Physiology* (pp. 31–68). Wiley. <https://doi.org/10.1002/cphy.c110001>

Shayman, J. A. (2000). Sphingolipids. *Kidney International*, *58*(1), 11–26. <https://doi.org/10.1046/j.1523-1755.2000.00136.x>

Shaughnessy, D.T., McAllister, K., Worth, L., Haugen, A.C., Meyer, J.N., Domann, F.E., Van Houten, B., Mostoslavsky, R., Bultman, S.J., Baccarelli, A.A., Begley, T.J., Sobol, R.W., Hirschey, M.D., Ideker, T., Santos, J.H., Copeland, W.C., Tice, R.R., Balshaw, D.M. & Tyson, F.L. (2014). Mitochondria, energetics, epigenetics, and cellular responses to stress. *Environmental Health Perspectives*, *122*(12), 1272–1278. <https://doi.org/10.1289/ehp.1408418>

Skorupa, M., Szczepanek, J., Mazur, J., Domagalski, K., Tretyn, A., & Tyburski, J. (2021). Salt stress and salt shock differently affect DNA methylation in salt-responsive genes in sugar beet and its wild, halophytic ancestor. *PLOS ONE*, *16*(5), e0251675. <https://doi.org/10.1371/journal.pone.0251675>

Smith, J., Sen, S., Weeks, R. J., Eccles, M. R., & Chatterjee, A. (2020). Promoter DNA Hypermethylation and Paradoxical Gene Activation. *Trends in Cancer*, *6*(5), 392–406. <https://doi.org/10.1016/J.TRECAN.2020.02.007>

Suzuki, M. M., & Bird, A. (2008). DNA methylation landscapes: provocative insights from epigenomics. *Nature Reviews Genetics*, *9*(6), 465–476. <https://doi.org/10.1038/nrg2341>

Tang, C. H., Hwang, L. Y., & Lee, T. H. (2010). Chloride channel CLC-3 in gills of the euryhaline teleost, *Tetraodon nigroviridis*: Expression, localization and the possible role of chloride absorption. *Journal of Experimental Biology*, *213*(5), 683–693. <https://doi.org/10.1242/jeb.040212>

Thorvaldsdottir, H., Robinson, J. T., & Mesirov, J. P. (2013). Integrative Genomics Viewer (IGV): High-performance genomics data visualization and exploration. *Briefings in Bioinformatics*, *14*(2), 178–192. <https://doi.org/10.1093/bib/bbs017>

Tine, M., Kuhl, H., Gagnaire, P.-A., Louro, B., Desmarais, E., Martins, R. S. T., Hecht, J., Knaust, F., Belkhir, K., Klages, S., Dieterich, R., Stueber, K., Piferrer, F., Guinand, B., Bierne, N., Volckaert, F. a M., Bargelloni, L., Power, D. M., Bonhomme, F., ... Reinhardt, R. (2014). European sea bass genome and its variation provide insights into adaptation to euryhalinity and speciation. *Nature Communications*, *5*(May), 5770. <https://doi.org/10.1038/ncomms6770>

Tipsmark, C. K., Baltzegar, D. A., Ozden, O., Grubb, B. J., & Borski, R. J. (2008). Salinity regulates claudin mRNA and protein expression in the teleost gill. *American Journal of Physiology. Regulatory, Integrative and Comparative Physiology*, *294*(3), R1004–14. <https://doi.org/10.1152/ajpregu.00112.2007>

Wang, J., Liu, W., Zhang, X., Zhang, Y., Xiao, H., & Luo, B. (2019). LMP2A induces DNA methylation and expression repression of AQP3 in EBV-associated gastric carcinoma. *Virology*, *534*, 87–95. doi:10.1016/j.virol.2019.06.006

Whitehead, A., Roach, J. L., Zhang, S., & Galvez, F. (2012). Salinity- and population-dependent genome regulatory response during osmotic acclimation in the killifish (*Fundulus heteroclitus*) gill. *Journal of Experimental Biology*, *215*(8), 1293–1305. <https://doi.org/10.1242/jeb.062075>

Yang, J., Liu, M., Zhou, T., & Lin, Z. (2023). Genome-wide methylome and transcriptome dynamics provide insights into epigenetic regulation of kidney functioning of large yellow croaker (*Larimichthys crocea*) during low-salinity adaptation. *Aquaculture*, *571*, 739410. <https://doi.org/10.1016/j.aquaculture.2023.739410>

Yu, G., Wang, L. G., Han, Y., & He, Q. Y. (2012). ClusterProfiler: An R package for comparing biological themes among gene clusters. *OMICS A Journal of Integrative Biology*, *16*(5), 284–287. <https://doi.org/10.1089/omi.2011.0118>

Zhang, Y., Zhu, F., Teng, J., Zheng, B., Lou, Z., Feng, H., Xue, L., & Qian, Y. (2022). Effects of salinity stress on methylation of the liver genome and complement gene in large yellow croaker (*Larimichthys crocea*). *Fish & Shellfish Immunology*, *129*, 207–220. <https://doi.org/10.1016/j.fsi.2022.08.055>

## Data Accessibility and Benefit-Sharing

Raw sequence reads (SRA) have been deposited at NCBI under Bioproject PRJNA952864.

#### Figure legends

Figure 1. A. Metagene profile of analyzed individuals from 2kb upstream of the Transcription Start Site (TSS) to 2 kb downstream of the Transcription End Sites (TES) B. Mean methylation profiles across genomic context centered on the *D. labrax* genome in freshwater- (FW) and seawater-acclimated fish (SW). All genomic regions were scaled to the same length.

Figure 2. Cluster analysis based on CpG methylation profiles in 5 freshwater-exposed (FW, black discs) and 5 seawater-exposed *D. labrax* (SW, white discs). A. Hierarchical clustering of samples was performed using Ward's method based on Pearson's correlation distance for cytosine CpG methylation. B. Principal Component Analysis (PCA) showing (PC1xPC2) coordination plane.

Figure 3. Cluster analysis based on gene expression levels in 5 freshwater-exposed (FW, black discs) and 5 seawater-exposed *D. labrax* (SW, white discs). A. Hierarchical clustering of samples was performed using Ward's method based on Pearson's correlation distance for gene expression levels. B. Principal Component Analysis (PCA) showing (PC1xPC2) coordination plane.

Figure 4. DNA methylation levels (in %) in different genomic context for different gene expression levels. Violin plots showing DNA methylation in promoter, first exon, first intron and gene body at different gene expression levels (divided into deciles based on increasing ranking of gene expression measured as log<sub>2</sub>-transformed normalized counts from DEseq2). Central red dots represent the median of the distribution. Correlations between DNA methylation and gene expression were measured using Spearman's rank correlation coefficient.

Figure 5. Genome-wide profile of CpG methylation. A. Chromosomal distribution of hyper- and hypomethylated regions in freshwater- compared to seawater exposed *D. labrax*. p-value < 0.05 and methylation difference [?] 25 %. B. Distribution of the differentially methylated regions (DMRs) in different genomic context. C. and D. Percentage of DMRs per exon and intron position normalized by the total size (in bp) of exons and introns respectively.

Figure 6. Enrichment analysis of genetic ontology (GO) terms. The 5 most significant GO terms for each group are represented. A. DNA methylome. B. RNA transcriptome. FW : fresh water; GB : gene body; PR : promoter; SW : seawater. The size of the dots represent the ratio of genes associated with the GO term and the colors indicate the p-values (threshold set at 0.05). Discussed GO terms are indicated by stars.

Figure 7. Venn analysis of methylome and transcriptome showing significantly overrepresented (p < 0.05) GO terms related to DEGs and DMRs (in genes and promoters) in FW vs SW conditions. A. Biological process. B. Molecular function. C. Cellular component. DMRs: differentially methylated regions ; DEGs: differentially expressed genes.

Figure 8. Comparison between freshwater (FW)-triggered gene expression changes and methylation changes in different genomic contexts. A: Proportion of down- and upregulated genes that are hypomethylated. B: Proportion of down- and upregulated genes that are hypermethylated. Blue color = downregulation in FW and red color = upregulation in FW.

Figure 9. Enrichment plot of the KEGG pathways enrichment analysis of differentially expressed and differentially methylated genes in promoters, first exons or first introns. The 5 KEGG pathways of each dataset displaying the most significant p-values have been represented. The proportion of clusters in the pie chart was determined by the proportion of genes in a specific category. The size of each circle represents the number of genes involved in each pathways (p-value < 0.05).

Table 1. List of selected differentially expressed and methylated genes

Figure 1S. Heatmap of significant differentially expressed genes across all samples with adjusted p-value < 0.05. Each row represents a differentially expressed gene between salinities arranged by ascending order of

fold change from top to bottom. The red and purple colors indicate the  $\log_{10}(\text{baseMean}+1)$  values. On the right, the colors indicate  $\log_2\text{FC}$  for downregulated genes (upper part of the figure, in light green) or upregulated genes (bottom of the figure, in red). Samples were visually clustered using hierarchical clustering. Dark green (top of the figure) = 5 SW individuals and purple = 5 FW individuals.

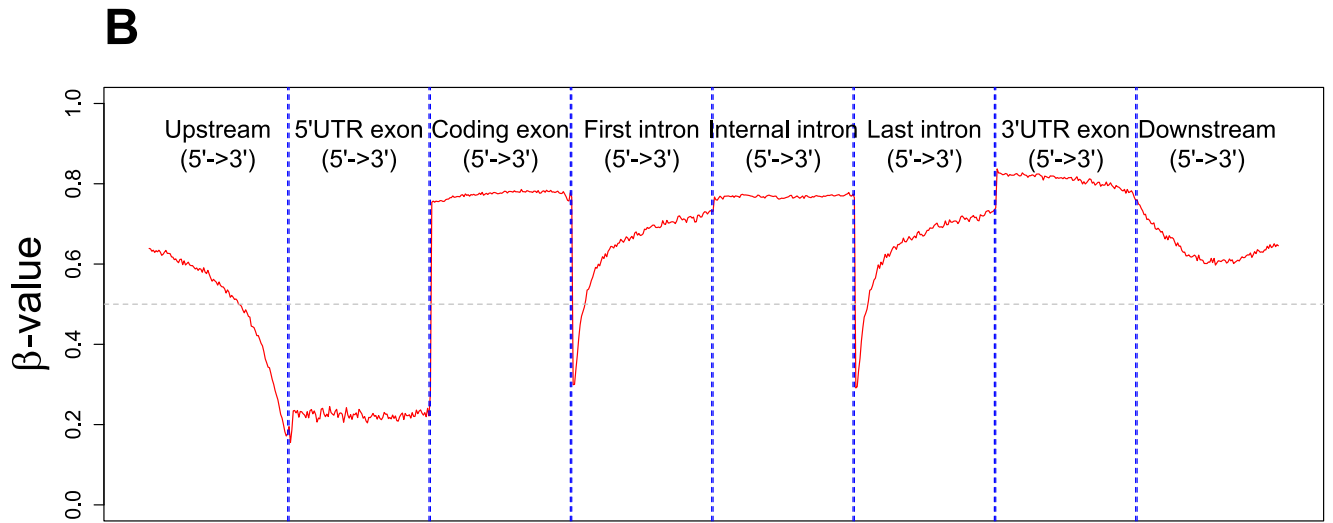
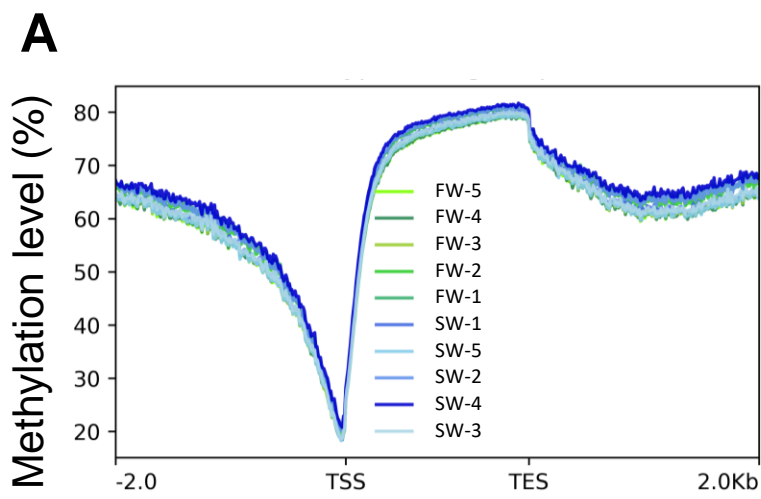


Figure 1. **A.** Metagene profile of analyzed individuals from 2kb upstream of the Transcription Start Site (TSS) to 2 kb downstream of the Transcription End Sites (TES) **B.** Mean methylation profiles across genomic context centered on the *D. labrax* genome in freshwater- (FW) and seawater-acclimated fish (SW). All genomic regions were scaled to the same length.

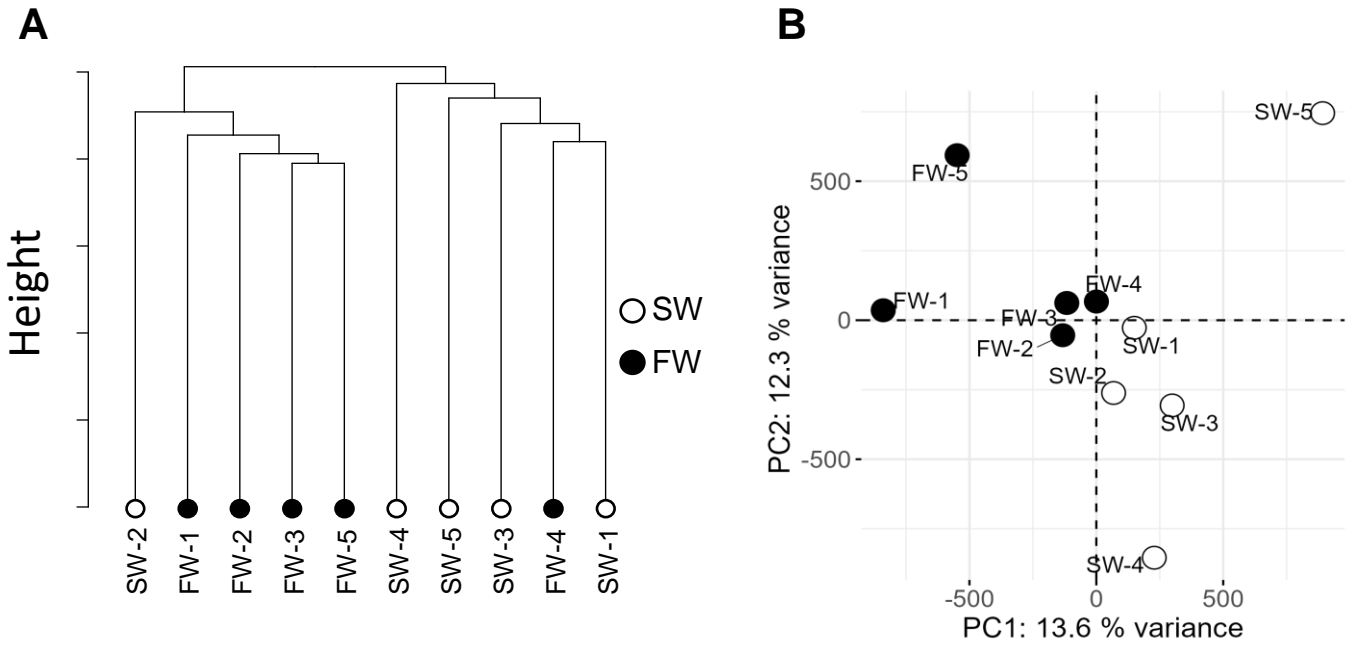


Figure 2. Cluster analysis based on CpG methylation profiles in 5 freshwater-exposed (FW, black discs) and 5 seawater-exposed *D. labrax* (SW, white discs). **A.** Hierarchical clustering of samples was performed using Ward's method based on Pearson's correlation distance for cytosine CpG methylation. **B.** Principal Component Analysis (PCA) showing (PC1xPC2) coordination plane.

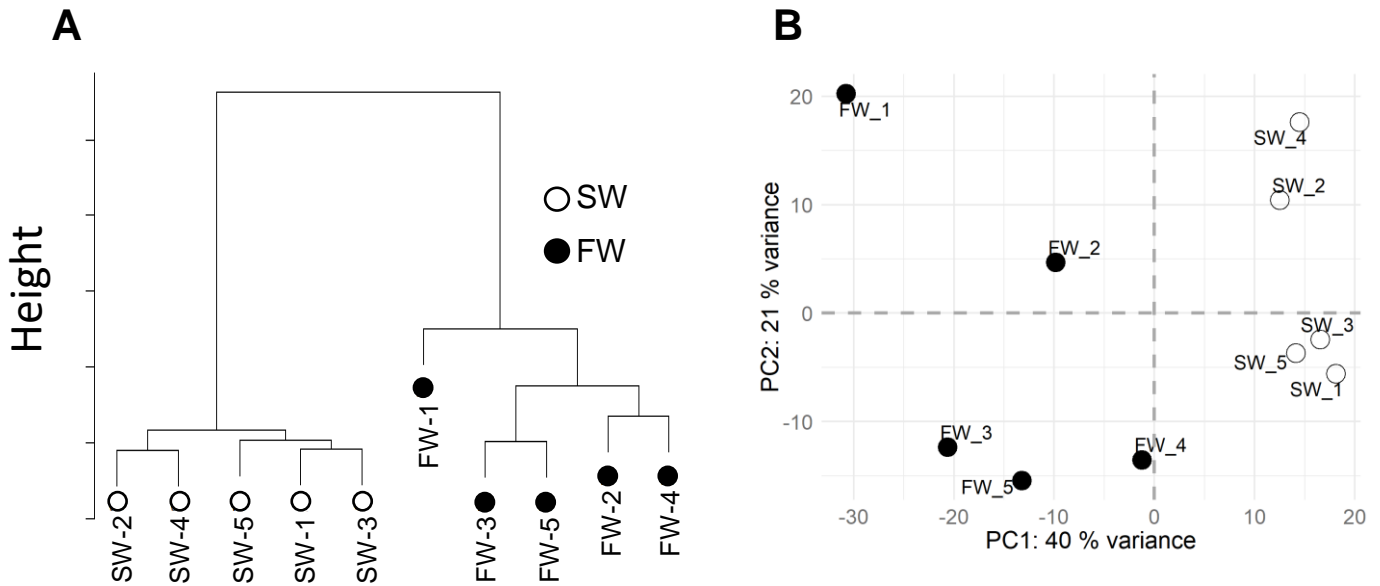


Figure 3. Cluster analysis based on gene expression levels in 5 freshwater-exposed (FW, black discs) and 5 seawater-exposed *D. labrax* (SW, white discs). **A.** Hierarchical clustering of samples was performed using Ward's method based on Pearson's correlation distance for gene expression levels. **B.** Principal Component Analysis (PCA) showing (PC1xPC2) coordination plane.

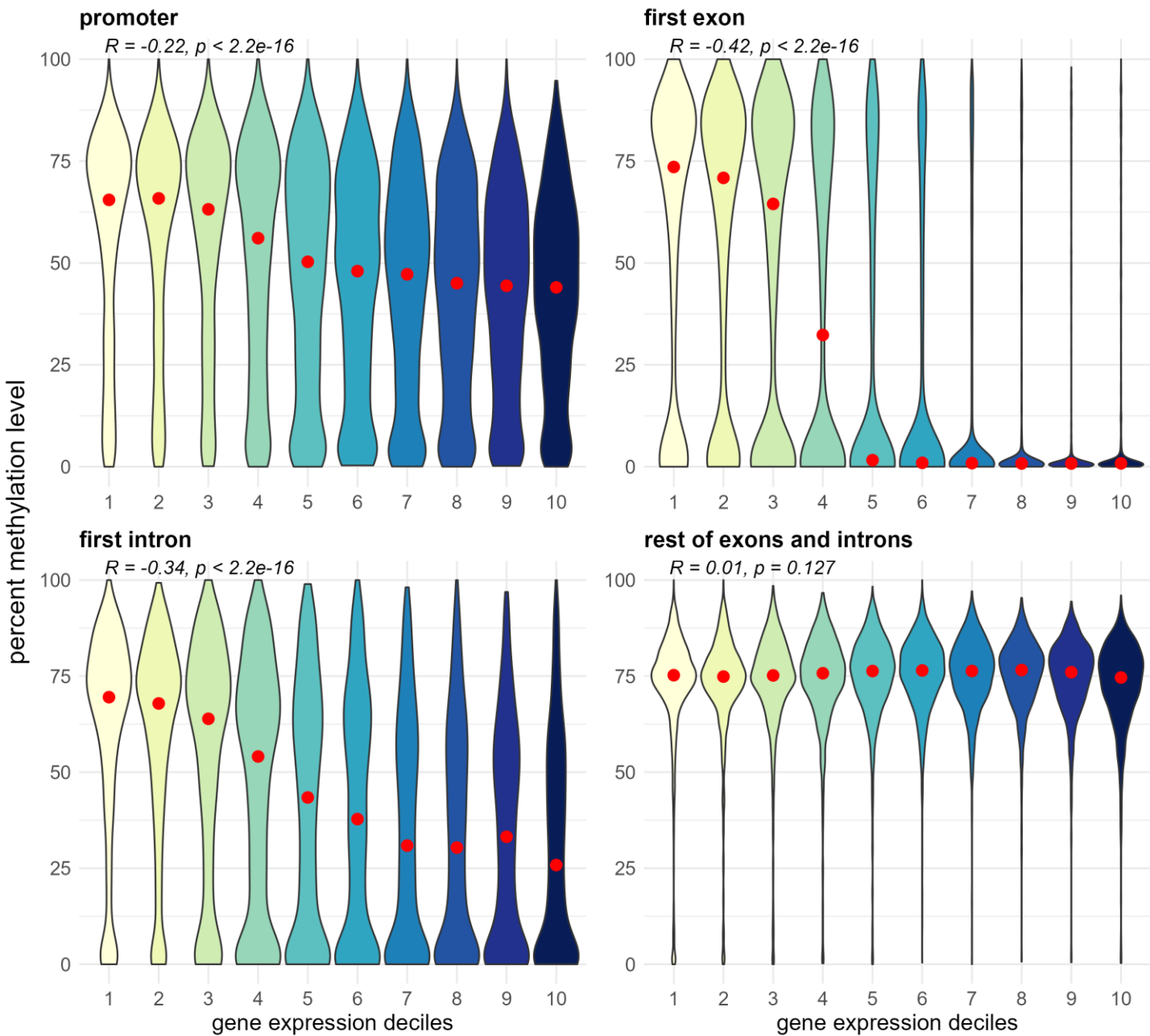


Figure 4. DNA methylation levels (in %) in different genomic context for different gene expression levels. Violin plots showing DNA methylation in promoter, first exon, first intron and gene body at different gene expression levels (divided into deciles based on increasing ranking of gene expression measured as log2-transformed normalized counts from DEseq2). Central red dots represent the median of the distribution. Correlations between DNA methylation and gene expression were measured using Spearman's rank correlation coefficient.

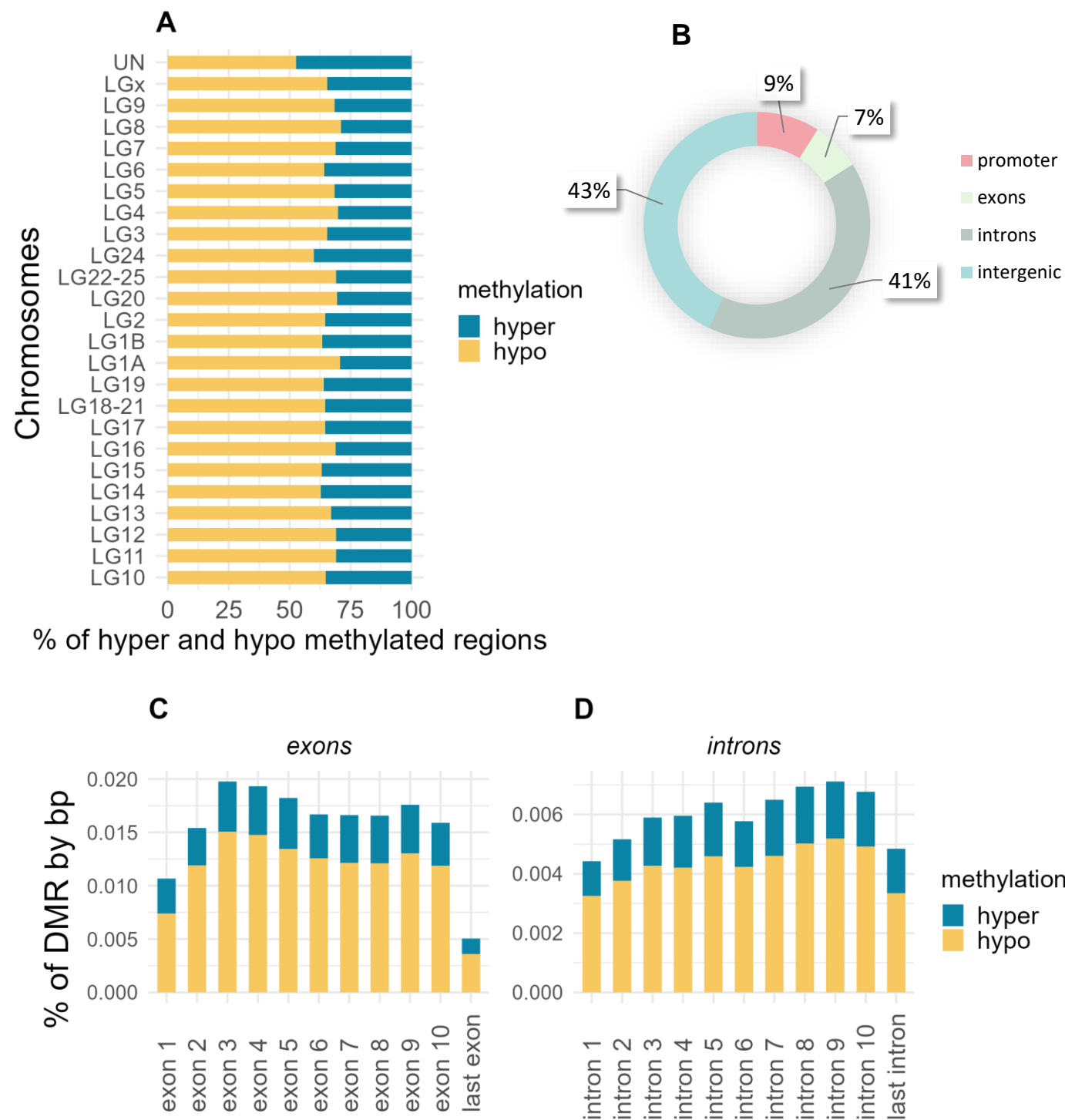


Figure 5. Genome-wide profile of CpG methylation. **A.** Chromosomal distribution of hyper- and hypo- methylated regions in freshwater- compared to seawater exposed *D. labrax*.  $p$ -value  $< 0.05$  and methylation difference  $\geq 25\%$ . **B.** Distribution of the differentially methylated regions (DMRs) in different genomic context. **C.** and **D.** Percentage of DMRs per exon and intron position normalized by the total size (in bp) of exons and introns respectively.

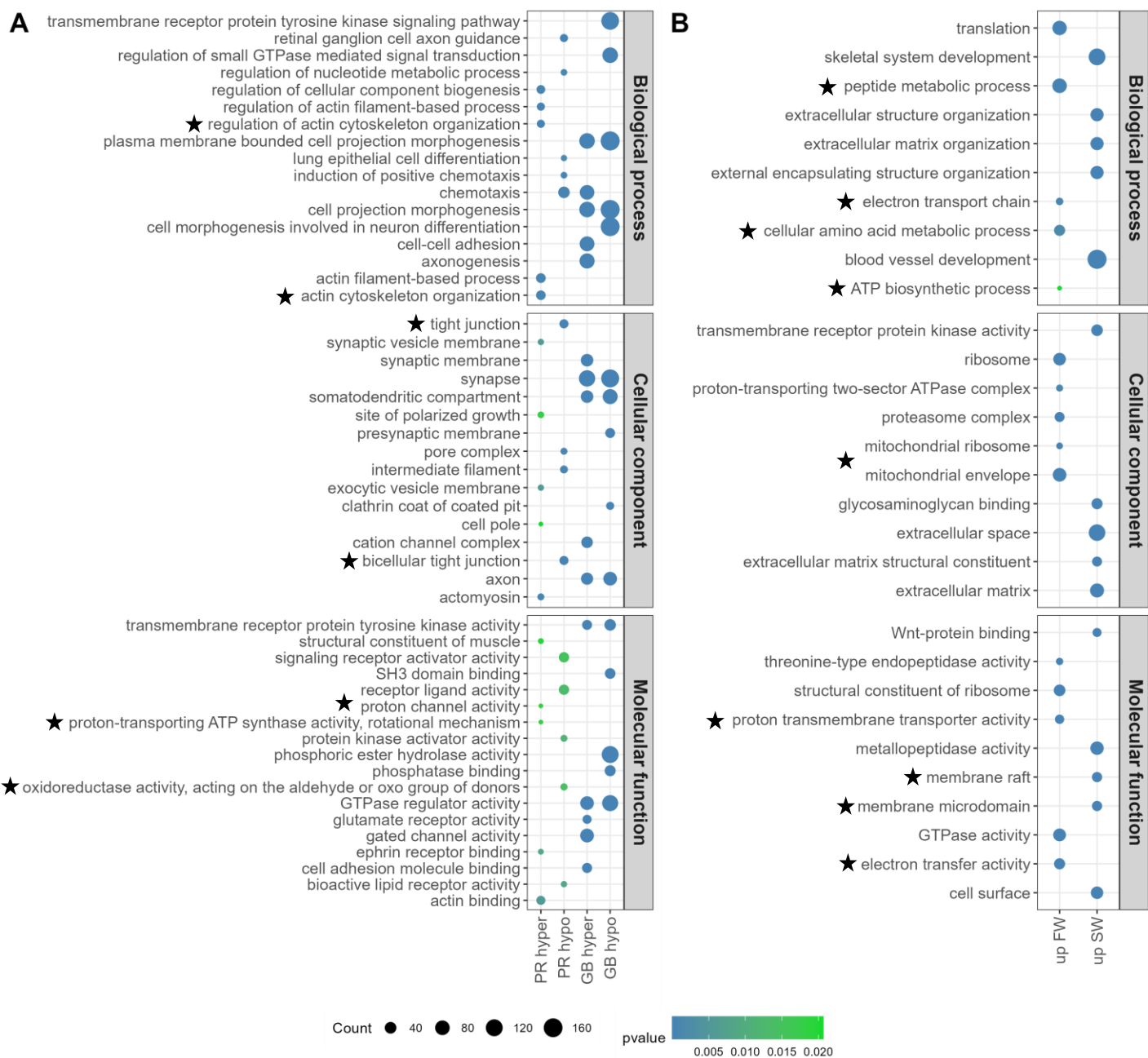


Figure 6. Enrichment analysis of genetic ontology (GO) terms. The 5 most significant GO terms for each group are represented. **A.** DNA methylome. **B.** RNA transcriptome. FW : fresh water; GB : gene body; PR : promoter; SW : seawater. The size of the dots represent the ratio of genes associated with the GO term and the colors indicate the p-values (threshold set at 0.05). Discussed GO terms are indicated by stars.

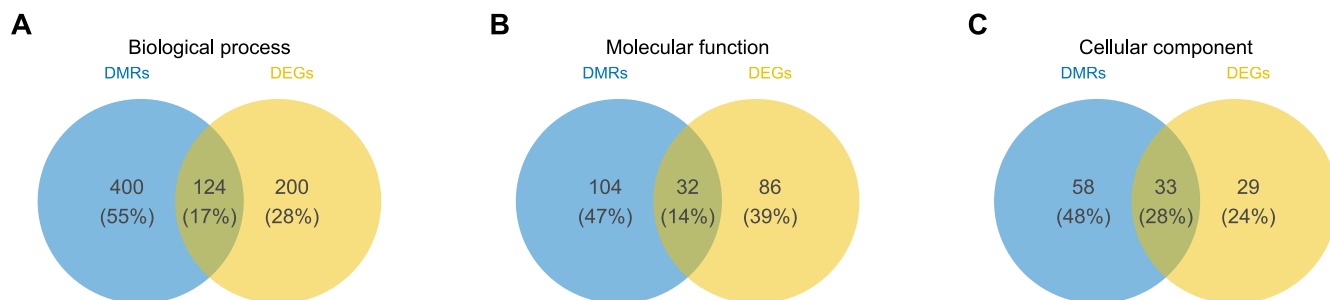


Figure 7. Venn analysis of methylome and transcriptome showing significantly overrepresented ( $p < 0.05$ ) GO terms related to DEGs and DMRs (in genes and promoters) in FW vs SW conditions. **A.** Biological process. **B.** Molecular function. **C.** Cellular component. DMRs: differentially methylated regions ; DEGs: differentially expressed genes.

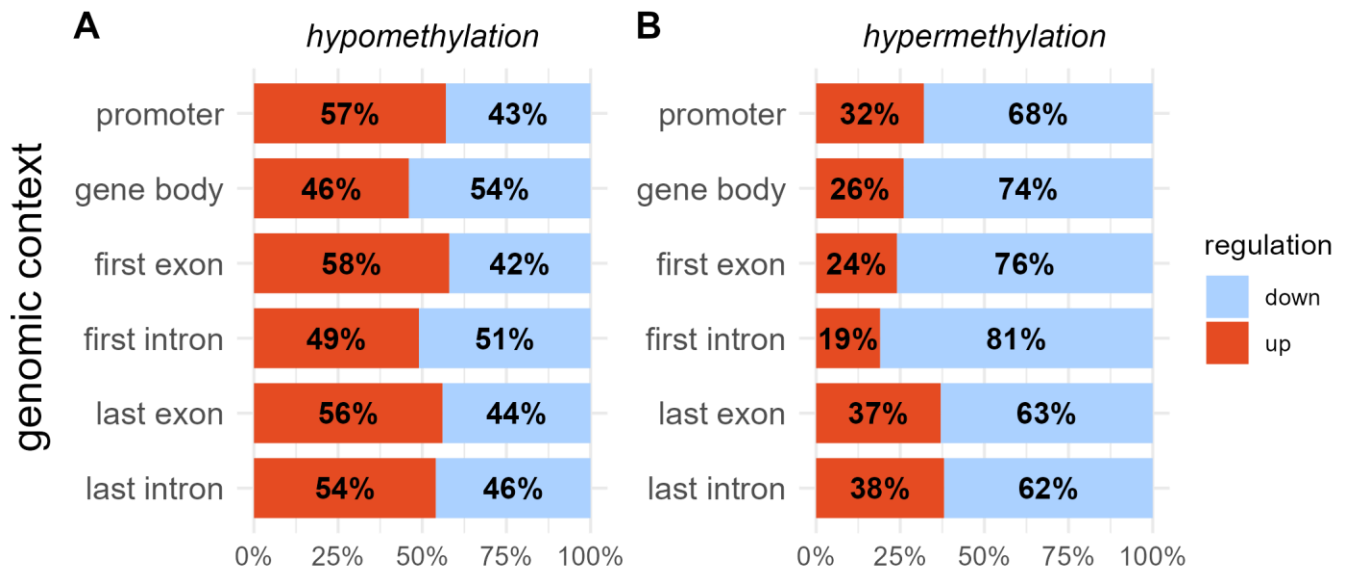


Figure 8. Comparison between freshwater (FW)-triggered gene expression changes and methylation changes in different genomic contexts. **A**: Proportion of down- and upregulated genes that are hypomethylated. **B**: Proportion of down- and upregulated genes that are hypermethylated. Blue color = downregulation in FW and red color = upregulation in FW.

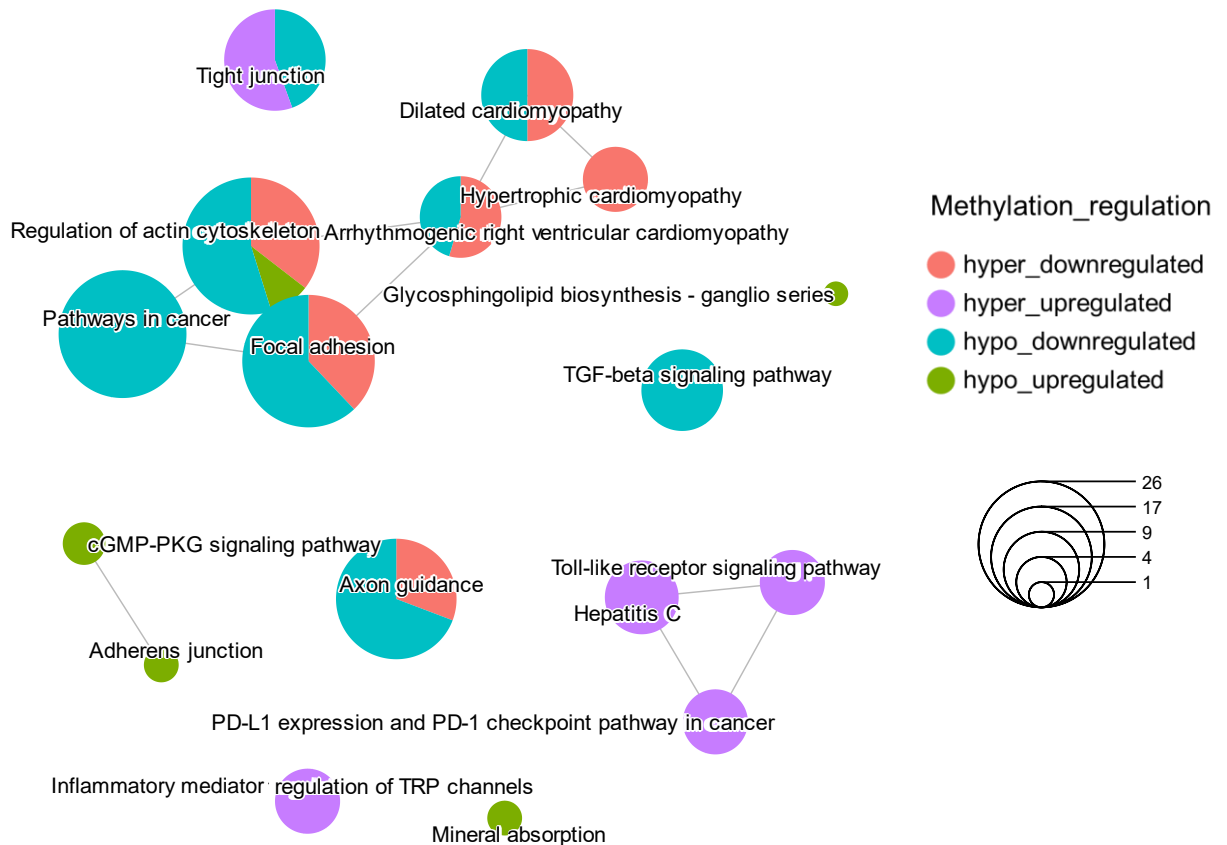


Figure 9. Enrichment plot of the KEGG pathways enrichment analysis of differentially expressed and differentially methylated genes in promoters, first exons or first introns. The 5 KEGG pathways of each dataset displaying the most significant p-values have been represented. The proportion of clusters in the pie chart was determined by the proportion of genes in a specific category. The size of each circle represents the number of genes involved in each pathways (p-value < 0.05).

Table 1. List of selected differentially expressed and methylated genes

Gene ID	Gene symbol	Gene expression (pval)	Methylation pattern (pval)	Position	Functions
DLAgn_00025050	<i>dnmt3a</i>	repressed (2.26E-3)	hypo (7.49E-3)	GB	DNA methylation
DLAgn_00069860	<i>dnmt3a</i>	repressed (2.87E-2)	hyper (8.39E-3)	GB	DNA methylation
DLAgn_00083540	<i>prlr</i>	induced (2.70E-2)	hypo (7.70E-5)	PR/GB	hormone receptor
DLAgn_00045010	<i>nr3c1 (gr)</i>	repressed (6.73E-4)	hypo (2.14E-4)	GB	hormone receptor
DLAgn_00137410	<i>atp1a1 (nka <math>\alpha</math>1a)</i>	induced (1.92E-3)	hypo (5.93E-3)	PR/GB	ion transporter
DLAgn_00058440	<i>atp1a3b (nka <math>\alpha</math>3)</i>	induced (3.35E-3)	hypo (3.94E-2)	PR	ion transporter
DLAgn_00174550	<i>atp2a2 (serca)</i>	repressed (3.84E-2)	hyper (2.30E-3)	PR/GB	ion transporter
DLAgn_00018050	<i>atp6v1b2 (vha)</i>	induced (2.93E-2)	hypo (3.54E-3)	GB	ion transporter
DLAgn_00070690	<i>atp6v1d (vha)</i>	induced (3.35E-4)	hypo (4.02E-2)	PR	ion transporter
DLAgn_00165220	<i>atp6v1e1b (vha)</i>	repressed (6.39E-3)	hypo (6.52E-3)	GB	ion transporter
DLAgn_00172160	<i>cfr</i>	repressed (3.52E-2)	hyper (1.58E-2)	GB	ion transporter
DLAgn_00005770	<i>clcn2</i>	repressed (7.48E-5)	hypo (4.39E-2)	GB	ion transporter
DLAgn_00028970	<i>clcn2</i>	induced (4.32E-10)	hyper (7.39E-3)	GB	ion transporter
DLAgn_00144740	<i>clcn3</i>	induced (6.18E-3)	hypo (2.12E-2)	GB	ion transporter
DLAgn_00027240	<i>kcnh5</i>	induced (1.38E-2)	hypo (1.33E-2)	GB	ion transporter
DLAgn_00019070	<i>kcnk5</i>	induced (1.44E-4)	hypo (1.45E-2)	PR	ion transporter
DLAgn_00102830	<i>kcnma1</i>	repressed (1.06E-3)	hypo (2.08E-2)	GB	ion transporter
DLAgn_00082860	<i>kcnt1</i>	induced (3.40E-2)	hypo (4.76E-2)	GB	ion transporter
DLAgn_00157760	<i>rhcg</i>	repressed (1.77E-2)	hypo (3.64E-2)	PR/GB	ion transporter
DLAgn_00214830	<i>scn4a (na<sup>+</sup> channel)</i>	repressed (1.56E-3)	hypo (3.53E-3)	GB	ion transporter
DLAgn_00080120	<i>slc12a2 (nkcc1)</i>	repressed (5.46E-13)	hyper (9.42E-4)	GB	ion transporter
DLAgn_00082210	<i>slc4a4a (nbc)</i>	repressed (5.29E-14)	hypo (2.51E-3)	GB	ion transporter
DLAgn_00044830	<i>slc9a6 (nhe6)</i>	induced (4.71E-3)	hyper (3.84E-2)	GB	ion transporter
DLAgn_00076860	<i>slc9a9 (nhe9)</i>	induced (1.99E-2)	hyper (2.54E-2)	GB	ion transporter
DLAgn_00117370	<i>aqp3a</i>	induced (1.15E-3)	hypo (1.38E-2)	PR/GB	water channel
DLAgn_00063040	<i>ptk2</i>	repressed (3.95E-3)	hypo (2.54E-4)	GB	transcription factor
DLAgn_00202150	<i>ptk2</i>	repressed (1.59E-19)	hyper (3.87E-2)	GB	transcription factor
DLAgn_00119940	<i>ostf1</i>	induced (7.75E-6)	hypo (4.48E-3)	GB	transcription factor
DLAgn_00088630	<i>cldn19</i>	repressed (5.41E-7)	hyper (2.94E-2)	GB	tight junction
DLAgn_00036050	<i>cldn4</i>	induced (5.73E-3)	hypo (1.63E-3)	PR	tight junction
DLAgn_00036080	<i>cldn4</i>	induced (3.82E-7)	hypo (9.15E-3)	PR	tight junction
DLAgn_00040400	<i>cldn7b</i>	induced (2.66E-3)	hypo (7.26E-4)	PR/GB	tight junction
DLAgn_00035230	<i>cldn8</i>	induced (3.99E-7)	hypo (1.57E-2)	PR/GB	tight junction
DLAgn_00035240	<i>cldn8</i>	induced (3.27E-2)	hypo (1.57E-2)	PR	tight junction
DLAgn_00036040	<i>cldna</i>	induced (6.95E-7)	hypo (1.63E-3)	PR/GB	tight junction
DLAgn_00044120	<i>cldnb</i>	induced (9.16E-5)	hypo (8.77E-3)	PR	tight junction
DLAgn_00143220	<i>cldnd</i>	induced (2.15E-5)	hypo (7.34E-3)	GB	tight junction
DLAgn_00087290	<i>tjp2</i>	induced (1.57E-2)	hypo (2.85E-3)	GB	tight junction
DLAgn_00124300	<i>tjp2</i>	repressed (4.59E-2)	hypo (4.74E-3)	GB	tight junction

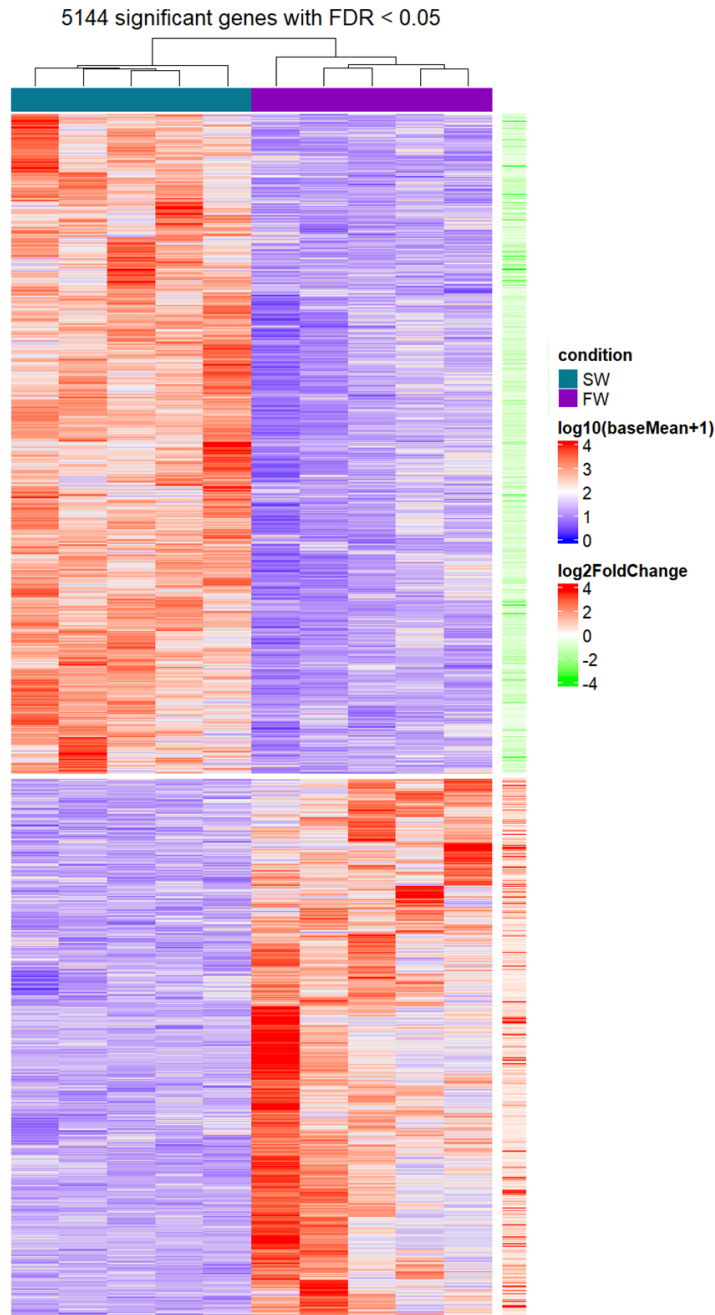


Figure 1S. Heatmap of significant differentially expressed genes across all samples with adjusted p-value < 0.05. Each row represents a differentially expressed gene between salinities arranged by ascending order of fold change from top to bottom. The red and purple colors indicate the log10 (baseMean+1) values. On the right, the colors indicate log2FC for downregulated genes (upper part of the figure, in light green) or upregulated genes (bottom of the figure, in red). Samples were visually clustered using hierarchical clustering. Dark green (top of the figure) = 5 SW individuals and purple = 5 FW individuals.